2020 Technology Research Review

February 4, 2020, Wanapum Dam Visitor's Center

Page No.	Time	Presenter	Project Title	Yrs
		Hanrahan	**Introduction**	
			Final Reports	
1	10:00	Jones	Development and validation of a precision pollination model	16-18
11	10:15	Whiting	Reducing cold damage with cellulose nanocrystals	18-19
18	10:30	Honaas	Enhancing reference genomes for cross-cultivar functional genomics	17-18
			Continuing Reports	
30	10:45	Good	Development of economical wifi-connected open-source sap flux probes: ***NCE***	18-19
37	11:00	Jones	Developing and validating models for tree fruit: ***NCE***	17-19
44	11:15	Kahani	Multi-purpose robotic system for orchards	18-20
53	11:30	Karkee	Towards automated canopy management in tree fruit crops: ***NCE***	18-19

FINAL PROJECT REPORT

Project Title: Development and validation of a precision pollination model

PI: Gloria DeGrandi-Hoffman
Organization: USDA-ARS Tucson
Telephone: 520-647-9187
Email: Gloria.Hoffman@ars.usda.gov
Address: Carl Hayden Bee Research Center
Address 2: 2000 East Allen Rd
City/State/Zip: Tucson, AZ 85719

Co-PI (2): Vincent P. Jones
Organization: WSU-TFREC
Telephone: 509-663-8181 x291
Email: vpjones@wsu.edu
Address: Dept. Entomology/TFREC
Address 2: 1100 N. Western Ave
City/State/Zip: Wenatchee, WA 98801

Co-PI (3): Tory Schmidt
Organization: WTFRC
Telephone: 509-665-8271 x4
Email: tory@treefruitresearch.com
Address: 1719 Springwater Ave
City/State/Zip: Wenatchee, WA 98801

Cooperators: Dr. Stefano Musacchi (WSU-TFREC), Karen Lewis (WSU-Extension), Dr. Melba Salazar-Gutierrez (WSU-Prosser), Dr. Lee Kalcsits (WSU-TFREC), Dr. Kirti Rajagopalan (WSU-Pullman).

Total Project Request: Year 1: $95,834 Year 2: $103,359 Year 3: $104,569

Percentage time per crop: Apple: 80 Pear: 0 Cherry:20 Stone Fruit: 0

WTFRC Collaborative Expenses:

Item	2016	2017	2018	**2019**
Salaries	5000	5000	5000	
Benefits	2000	2000	2000	
Wages	8000	12,000	12,000	
Benefits	2400	3600	3600	
RCA Room Rental				
Supplies				
Travel	1800	2000	2000	
Miscellaneous				
Total	19,200	24,600	24,600	**0**

Budget 1
Organization Name: USDA-ARS **Contract Administrator:** Laura Elmore
Telephone: 520-647-9160 **Email address:** Laura.Elmore@ars.usda.gov

Item		2017	2018	**2019**
Salaries		$1000	$1000	**0**
Benefits				
Wages				
Benefits				
Equipment				
Supplies				
Travel		$4,000	$4,000	**0**
Plot Fees				
Miscellaneous				
Total			$5,000	**0**

Footnotes:

Organization: WSU-TFREC **Contract Administrator**: Katy Roberts/Shelli Thompkins
Telephone: 509-335-2885/509-293-8803 **Email:** arcgrants@wsu.edu / shelli.tompkins@wsu.edu

Item	2016	2017	2018	**2019**
Salaries[1]	35,000	45,000	46,800	**0**
Benefits[1]	15,120	11,493	11,953	**0**
Wages[2]	18,800	11,440	11,898	**0**
Benefits[2]	1,214	309	321	**0**
Equipment				
Supplies	3,500	3,500	2,500	**0**
Travel[3]	3,000	1,500	1,560	**0**
Miscellaneous				
Plot Fees				
Total	76,634	73,242	75,032	**0**

Footnotes:
[1] Salaries and benefits are for a half-time grant manager
[2] Wages and benefits are for student temporary employees.

Objectives:

1. Update DeGrandi-Hoffman's original apple bloom phenology model to incorporate newer cultivars and horticultural advances.
2. Examine the effects of netting on honey bee foraging and modify foraging model accordingly.
3. Incorporate information on honey bee foraging and cross-pollination rates into the pollen tube growth model to improve decision making and thinning practices. Also evaluate foraging model on cherry.
4. Evaluate the effects of variability in spring weather conditions, as well as directional shifts toward earlier bloom, on fruit set and best pollination management strategies.

Significant Findings:

- Timing of full bloom is predictable for seven new cultivars: Cosmic Crisp, Fuji, Gala, Granny Smith, Jonagold, Golden Delicious, and Honey Crisp.
- Netting slows the progression of bloom compared to no nets, reduces the abundance of honeybees foraging, and results in lower and more variable fruit set.
- Honeybee foraging is driven by the number and relative abundance of open flowers on the mix of cultivars open at any time throughout the bloom period.
- Fruit set is completed in a fairly narrow window with 5% fruit set by 350 DD and 95% by 425-450 DD.
- Our fruit set model shows that the latter roughly 24% of flowers only contribute about 5% to the fruit set observed in our studies.
- Evaluation of the effect of climate change scenarios on honeybee foraging showed that temperatures during the bloom period will have a minor effect on foraging rates. However, the shorter daylength and lower intensity of sunlight occurring earlier in the year, when apples will bloom in Washington, will cause up to 20% reduction in foraging efficiency.

Obj. 1. Update DeGrandi-Hoffman's original apple bloom phenology model to incorporate newer cultivars and horticultural advances.

Materials and Methods: The past four years, we collected bloom phenology data at the WSU Sunrise orchard from six different cultivars (Fuji, Gala, Golden, Granny Smith, Jonagold, and Cosmic Crisp, Honeycrisp (2019 only)) and also analyzed data collected in 2016 from Honeycrisp and Gala (Honeycrisp were collected from two locations, Gala from one). Data collection focused only on the bloom period and we counted the number of blooms open at each visit on a given number of branches on a particular number of trees rather than following a smaller number of marked buds. This gives a much larger number of blooms at any point in time and seemed to define the bloom period much better. Analysis was done by examining the fit to five different statistical distributions and choosing the one that gives the best fit to the observed data.

Fig. 1. Probability density functions for the different numbers of open flowers.

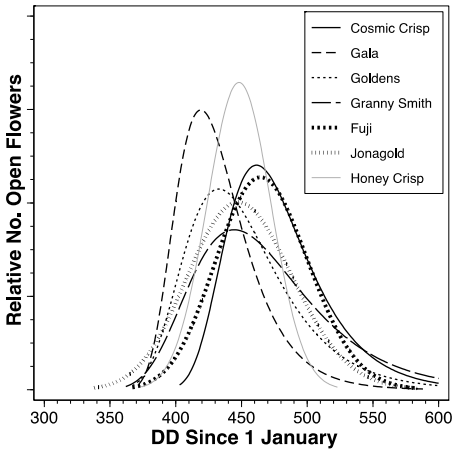

Results: We have analyzed the data for bloom for all cultivars and have well defined the bloom period for each of the cultivars (Fig. 1). The models on DAS will be updated with the newest models based on our data for the last four year. These values have also been used in our fruit set model (objective 3).

Objective 2. Examine the effects of netting on honey bee foraging and modify foraging model.

Methods: Two adjacent blocks of Fuji's were used for this study. One block had overhead nets deployed before bloom while the other block was not covered with overhead netting throughout the study. The study utilized the entire 9 acre "no-net" block and ≈10 A of the 24 A block covered with netting. Trees in both blocks were trained on trellises. The net was a white 20% light-reducing netting that extended down over the top wires about 2 ft along the sides, 4 ft down along the front and all the way to down to the ground on the back (west side).

Bloom progression assessment: The blossoms were hand-thinned to about one flower per spur at the start of bloom in each block. In each block, three sections along the trellis were marked and each section contained ≈200 flower buds. The number of flowers observed for bloom progression was 618 and 610 flowers in the net and no-net blocks, respectively. The number of open flowers were recorded each time the flowers were observed, and these data was used to estimate % bloom.

Honeybee abundance: On April 4, four sets of four hives were placed under the nets next to the trees on the west side of the netted block and two sets of four hives were placed along the east edge of the block with no nets. The abundance of honey bees foraging in each block was assessed by slowly walking down a row and counting bees observed on or near apple trees during five-minute intervals. Three to six 5-min observations were made in each block on the days foraging bees were counted. All counts made within a block were averaged on a daily basis.

Fruit set: Transects were set up along the entire length of seven rows in each block and each transect contained five trees that were used for estimating fruit set (n = 35 trees per block). Distances for trees located along each transect were 40, 200, 360, 600 and 760 ft from the side of each block where the bee hives were located. The length of each tree row was ≈ 800 ft and the trees closest to the edges of the blocks were located 40 ft in from the edges.

Results: We observed several differences between the net and no-net blocks. First was that bloom progressed earlier in the no-net block compared with bloom under netting (Fig. 2a). Fifty percent bloom occurred on 27 Apr in the no-net block compared with 29 Apr for 50% bloom under nets. We also observed considerably more honeybees foraging in apple trees without nets compared with the amount observed foraging under nets (Fig. 2b). When we standardized the number of bees per open blossom, we saw that the abundance of bees per open blossom was always higher in the block without nets (2c). Fruit set was more uniform (between 60-80%) along transects in the no-net block compared with the uniformity of fruit set observed under nets (15-80%) (Fig. 3). Fruit set in the block covered with nets decreased along the transects from the edges into the interior of the block.

Fig. 2. Effect of netting on flowering and honeybee foraging. A) Progression of flowering. B) Number of honeybees observed in 5 minute samples. C) Average number of honeybees per open flower.

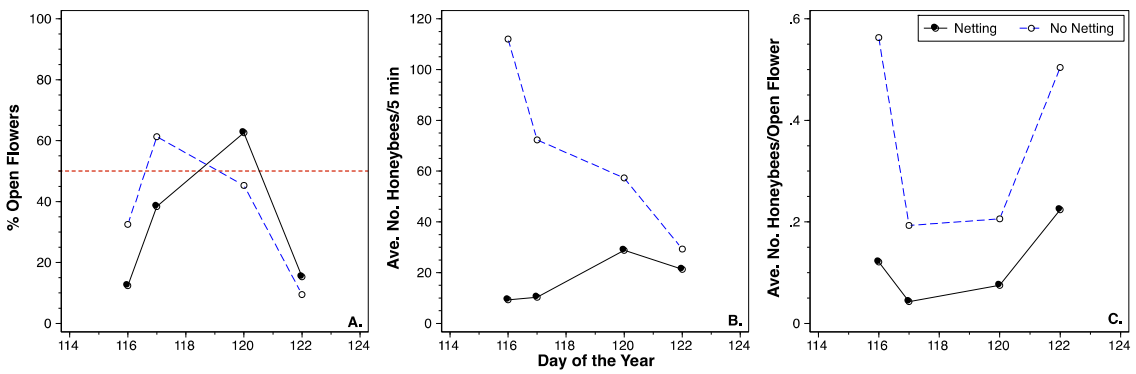

We also saw additional ways that nets impacted pollinators. Bees often fly up and out when leaving an area. In this study, we observed that wild bees, bumble bees and honey bees became trapped in the upper corners where the nets were folded over the top wires. This resulted in exhaustion of the bees and an accumulation of dead and dying bees on the ground under the corner. It appears that having the edge of the net folded down over the top wire prevented some bees from leaving the netted area. One possible solution would be to install the nets so that they are flat. However, bees often were seen flying up and bouncing off the interior net ceiling indicating that nets inhibit upward flight of honey bees. Overall, orchard netting appears to negatively impact honey bee flight during bloom and subsequent fruit set.

Fig.3. Effect of netting on fruit set.

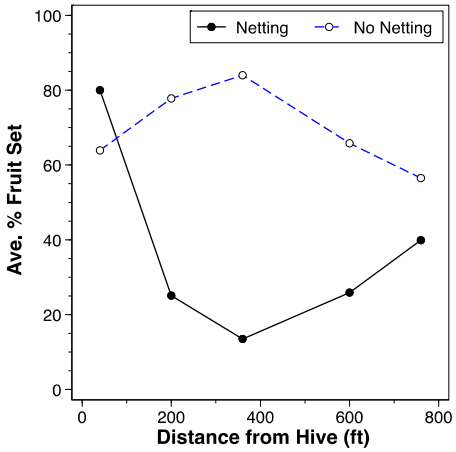

Obj. 3. Incorporate information on honeybee foraging and cross pollination rates into the pollen tube growth model to improve decision making and thinning practices. Evaluate foraging on cherry.

Methods Cultivar Choice and Fruit Set: The evaluation of flowering is discussed in objective 1, but those data were also used to calculate the relative proportion of flowers that were open for the different cultivars throughout the bloom period (Fig. 4.) The proportion of open blossoms for each cultivar includes data from figure 1, and the relative abundance of the different flowers in our plots. That data was paired with the foraging rates (number of bees on each cultivar) that were taken every few hours throughout the foraging periods.

We also did some studies on fruit set involving the four cultivars Fuji, Golden, Granny, and Jonagold; we were not allowed to do any thinning of the Cosmic Crisp in either the location at Sunrise or in

Fig. 4. The proportion of total open flowers each cultivar comprises throughout the bloom period. Based on data from figure 1

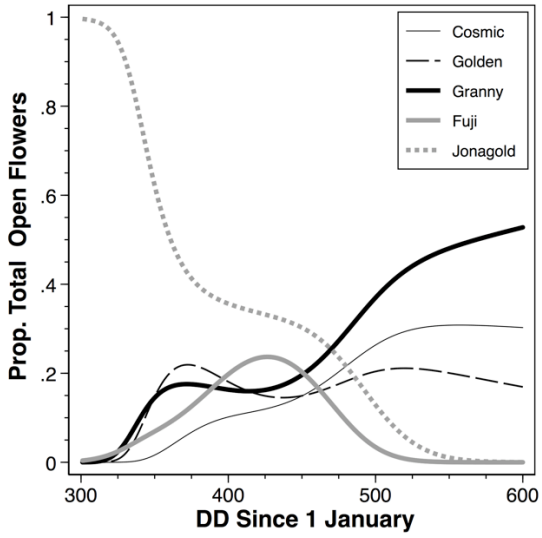

Fig. 5. Correlations between the relative number of open blooms (solid line) and the proportion of honeybees foraging each date on that cultivar.

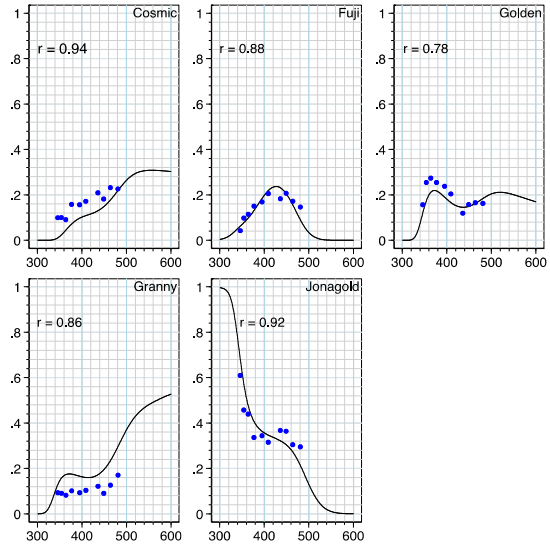

Quincy, so we have fruit set if no thinning occurred, but nothing else for that cultivar. Hand thinning happened on April 24, 26, 28, and May 1st. These thinning dates corresponded to 337, 416, 459, and 504 DD. The "no thinning" count was done on 24 April, but assumption is that this happened at the end of the flowering period or ≈ 600 DD.

Methods Cherry Flowering Time: The cherry flowering was investigated in 2018. We were able to determine the bloom phenology of Chelan cherries at a single location near Rock Island. The overlap of bloom in apples and cherries made it nearly impossible to sample both and the choice of apples as being more important was based on the larger amount of data that we had and felt that we could finish up this past year. We did not do more cherry work as Dr. Mike Willett indicated at the last technology review that cherry bloom work had been completed at the OSU Hood River Station and not to pursuit this further.

Fig. 6. Bloom curve (solid line) and fruit set when all open flowers were removed at five different times of the season for four different apple cultivars

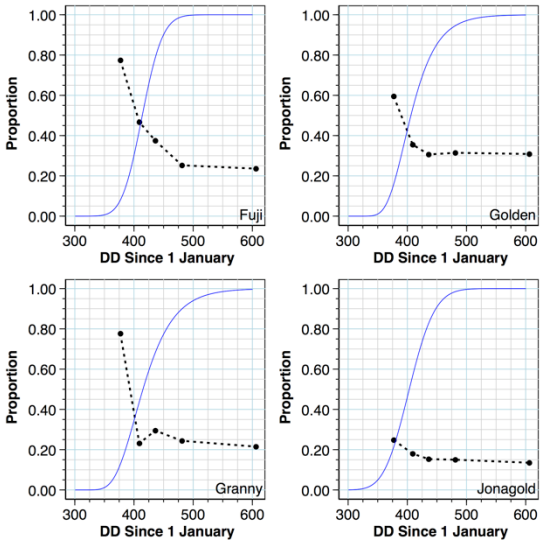

Results Cultivar Choice by Honeybees: The data showed that the honeybee distribution on the different cultivars was highly correlated to the relative proportion of flowers that were in bloom (Fig. 4). The correlations were very good and support the idea that the honeybees do not actively discriminate among cultivars, instead their distribution is related to the numbers of flowers that are open on a particular cultivar at any given time. While there were some differences where the number of bees (dark dots) were higher than the proportion of flowers open on Cosmic Crisp (Fig. 5) – this is likely due to the Cosmic Crisp block being closest to the large bee yard. Similarly, the Granny area sampled for bees was the location that was farthest from any of the hives, whereas Fuji, Golden, and Jonagold were about the same distance from the hives and track the bloom density curve very well.

Fig. 7. Proportion final fruit set (open circles) and proportion bloom completed (solid circles) for each of four cultivars tracked at the Sunrise orchard in 2018.

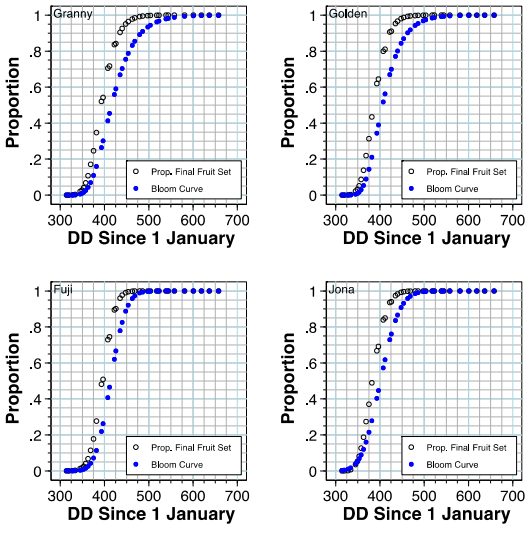

Results Fruit Set: The fruit set was highest early in the bloom period for all cultivars, then tended to flatten out by the second time the flowers were thinned (Fig. 6). The exception to this was Fuji whose flowering tends to start and peak later than the other cultivars – that cultivar didn't flatten out until the last hand thinning on 1 May. Jonagold, which starts blooming early and comprises the majority of the cultivars in our blocks showed very little variation in fruit set throughout the season. This is because early on, the majority of the flowers open were other Jonagold flowers, so that the cross-pollination rates for that cultivar were very low initially, and throughout the majority of the flowering period (until about 460 DD).

When the bloom curve (blue dots – cumulative proportion of all flowers open) is plotted on the

same axis as the cumulative proportion of all fruit set (Fig. 7), we found the latter 24% of the flowers from Jonagold only contributed about 5% of the total fruit set for that cultivar. Virtually the same percentages were also found for the other 3 cultivars (24.5, 23, and 23% for Granny, Golden, and Fuji's, respectively). You can see in the difference is that the latter flowers really play almost no role in fruit set.

Examination of the model output also showed that the window for setting fruit is fairly narrow; the center 90% of all fruit are set within 75 to 100 DD. For all 4 cultivars fruit set reached around 5% fruit set at 350 DD and 95% fruit set between 425-450 DD.

Obj. 4. Evaluate the effects of variability in spring weather conditions, as well as directional shifts toward earlier bloom on fruit set and best pollination management strategies.

Evaluation of bloom time was presented in last year's progress report and showed that at three representative locations (Richland, Wenatchee, Wapato) median bloom time (median is when half the years evaluated will be above and half below all bloom time values) will be changed by 21 days using the mild scenario (RCP 4.5 -up to 650 ppm CO_2 with stabilization after 2100) and 30 days using the increasingly more likely climate change scenario (RCP 8.5 – 1380 ppm CO_2 and still rising at 2100.

The earlier flowering time poses several possible problems for honeybee pollination. First, bloom starts earlier in the year which means that the day length occurring at those earlier dates will reduce honeybee foraging time (since they only forage during the day). Secondly, the sunlight is less intense early in the season, which also affects foraging rates. Third, the temperatures around the bloom period may be more variable with either higher or lower temperature profiles during the day. The temperature profile is also a key driver of honeybee foraging and could affect foraging either positively or negatively. The fourth potential issue is that Washington tree fruit is not the only crop that is affected by climate change and it is likely that crops like almonds that bloom earlier in the year will also be shifted. At first glance, it might seem the shift in almonds will not be a problem, because we use the same bees that pollinate California almonds. However, population growth in honeybee colonies is driven by day length. Egg laying by queens does not occur until day lengths reach 10-11 hours photoperiod. Thus, we might not have well developed colonies (with large amounts of brood from pollination of almonds) to the extent that we currently enjoy.

*Methods***:** To test the first two issues, we used data gathered the past two years for bloom timing of Cosmic Crisp (very late blooming) and Jonagold (very early blooming) and examined the period between 5% flowering of Jonagold and 95% flowering of Cosmic Crisp. We used the same climate change scenarios for the same three locations (Richland, Wenatchee, Wapato) as before and added another one (Oroville) to examine how much the temperatures and reduced sunlight might affect honeybee foraging rates across the north-south extent of Washington tree fruit production. As before, we used the periods for historical (1979-2005), 2040 (2025-2055), 2060 (2045-2075), and 2080 (2065-2095) using the two climate change scenarios.

Results: We found that the median temperature profile during the bloom period did not vary more than 1.2°F at any site with either climate change scenario. These relatively small temperature changes during the bloom period resulted in about the same performance in honeybees foraging, with only a slight change (max < 3.4%) in foraging rates related to temperature. Essentially, even though the bloom period occurs much earlier on a calendar date basis, the temperature profiles will not vary enough to effect honeybee foraging.

In contrast to the temperature effects, the median sunlight duration at the earlier dates of bloom vary from ≈1.1-1.6 hours less (RCP8.5) or 1-1.3 hours (RCP4.5) less with the reduction increasing from

Oroville to Richland. These values correspond to a reduction in foraging time of 7.5-10.9% or 6.4-9.5% for the more severe and less severe scenarios, respectively.

In addition to reduced foraging times because of the earlier flowering times, the sunlight intensity at any given time is also affected by day of the year and is reduced early in the year compared to the historical foraging time. The differences in sunlight intensity from bloom occurring earlier in the year causes about a 4-10% reduction in foraging rates compared to the historical normal bloom period (this is based on the clear sky radiation, so it doesn't consider any change in cloud cover that is not predictable). Overall, the reduction in foraging caused by changes in both sunlight duration and intensity amounts to roughly 10.4-17.4 and 11.4- 20.1% reduction (RCP4.5 and RCP8.5, respectively) compared to the historical time of bloom. All of these effects are smallest in the more northerly locations and increase going south and as time goes on.

Fig. 8. Change in honeybee foraging rate caused by shift in time of bloom which causes foraging to occur under less intense sunlight and shorter days. RCP4.5 is mild climate change scenario, RCP8.5 is the more severe situation.

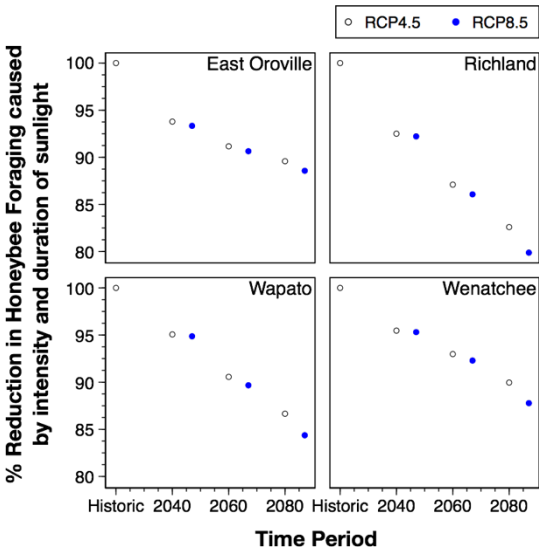

The changes in honeybee foraging related to climate change appear to be primarily a result of the shorter day length and lower intensity of sunlight earlier in the season. The climate change scenarios do not provide any indication of cloudiness, so our study assumes the clear sky radiation value and how that changes over the year. If there are any differences that are systematic (*e.g.,* earlier days are cloudier as the climate changes), then the effects may be greater or lesser than what our study suggests. Regardless, the changes should occur relatively slowly, but the expectation should be that the bees will be less efficient (up to ≈20%) which would require more bees to achieve the same results as we have currently. Another way to view this is from the perspective of "climate analogs", where we look at a location in the future and compare it a current location. In this sense, the flowering time in Oroville will be similar to the Richland location in 2080 under the RCP4.5 and in 2060 under RCP8.5. Similarly, in 2040 Wenatchee will have the same median flowering time as Richland currently does under either climate change scenario.

Executive Summary

Project Title: Development and validation of a precision pollination model

Keywords: apple bloom curves, netting effects on honeybees, climate change effects on pollination, fruit set model

Abstract: Bloom curves for 7 different apple cultivars were developed. Netting during bloom slows bloom, disorients honeybees, and reduces both pollination and fruit set. A fruit set/pollination model shows that the first 95% of fruit set happens within the first 75% flowering. Climate change will reduce honeybee efficiency between 11.4-20.1%.

Summary: We developed bloom curve models to predict when bloom occurs on a degree-day basis for the cultivars Fuji, Gala, Golden Delicious, Granny Smith, Jonagold, Cosmic Crisp and Honeycrisp. These models are useful in timing predictions, but also understanding the overall pollination/fruit set system and in models for fruit set.

We also evaluated the effects of netting being up during the bloom period. We found that the netting slowed the process of bloom, reduced the number of honeybees foraging under netting, and made fruit set much more erratic than in open areas. We also found that if the edge of the netting was dropped down slightly from the top (*e.g.,* a foot), that the honeybees tended to get caught in the area and die of exhaustion because they couldn't return to the hive and couldn't escape.

Evaluation of the honeybee foraging patterns on different showed that they were determined by the relative abundance of the flowers compared to the other cultivars – the more flowers present on a particular cultivar was highly correlated to the number of honeybees foraging there. We also found that a modified version of Dr. DeGrandi-Hoffman's model predicting fruit set tracked well with our field studies where we examined fruit set in manipulated plots (where we thinned or not at different times throughout bloom). Further examination suggests that the first 75% of the bloom period is responsible for 95% of the fruit set and that most of the fruit set occurs in the period of 350-450 DD.

The effect of climate change was evaluated using climate change scenarios and the honeybee foraging model currently on WSU-DAS. This model is a variation of Dr. DeGrandi-Hoffman's foraging model and allows us to evaluate the quality of foraging based on temperature, wind speed, solar radiation, and rainfall. For our simulations, we only incorporated climate change scenarios for temperature and solar radiation, since rainfall and windspeed are not well predicted by the climate change scenarios. We found that bloom should occur between 21-30 days earlier by 2080, but the temperature profile during the bloom period would change only slightly (1.2°F), which would have minimal impact on honeybee foraging. However, the earlier bloom dates would decrease the median daylength between 1.1-1.6 hours (using the most likely scenario) or 7.5-11%. Moreover, the median intensity of sunlight also would be reduced so that overall we expect foraging would be reduced from 11.4-20.1% depending on the location and time frame examined. These effects could be much worse if there is some systematic change in windspeed or rainfall that would occur in the earlier times. Note these effects do not consider how the honeybee colony health and population dynamics would be affected by climate change, which is being examined in another grant (not funded by the commission).

FINAL PROJECT REPORT

Project Title: Reducing cold damage with cellulose nanocrystals

PI: Matthew Whiting
Organization: WSU-IAREC/CPAAS
Telephone: 509-786-9260
Email: mdwhiting@wsu.edu
Address: IAREC
Address 2: 24106 N. Bunn Road
City/State/Zip: Prosser/WA/99350

Co-PI (2): Changki Mo
Organization: WSU-Tricities School of MME
Telephone: 509-372-7296
Email: changki.mo@tricity.wsu.edu
Address: WSU-Tricities
Address 2:2710 Crimson Way
City/State/Zip: Richland/WA/99354

Co-PI(3): Xiao Zhang
Organization: Chem. Eng., WSU
Telephone: 509-372-7647
Email: xiao.zhang@tricity.wsu.edu
Address: Ctr for Bioproducts & Bioenergy
Address 2: 2710 Crimson Way
City/State/Zip: Richland/WA/99354

Co-PI (4): Bernardita Sallato
Organization: WSU-Extension
Telephone: 509-439-8542
Email: b.sallato@wsu.edu
Address: IAREC
Address 2: 24106 N. Bunn Road
City/State/Zip: Prosser/WA/99350

Cooperators: Olsen Brothers, Zirkle Fruit Co.

Percentage time per crop: Apple:50 Pear: Cherry:50 Stone Fruit:

Other funding sources

Agency Name: USDA NIFA AFRI Bioenergy
Amt. requested/awarded: $404,030
Notes: Funded for 2018-2021 to investigate cellulose nanocrystal suspension preparation, thermal properties, field trials with CNC

Agency Name: WSU Commercialization Gap Fund
Amt. requested/awarded: $50,000
Notes: this funding is to evaluate plant-based dispersions for reducing cold damage, protect the IP, and develop a business plan for the commercialization of the IP

Total Project Funding: $92,736

Budget 1
Organization Name: WSU **Contract Administrator: Katy Roberts**
Telephone: 509-335-2885 **Email address: arcgrants@wsu.edu**

Item	2018	2019
Salaries	31,471	32,730
Benefits	2,360	2,455
Wages	4,800	4,992
Benefits	455	473
Equipment		
Supplies	10,000	1,000
Travel	1,000	1,000
Plot Fees		
Miscellaneous		
Total	50,086	42,650

Footnotes: salary for graduate research assistant to work out of WSU-IAREC; wages are to support hourly employees to assist with field trials and hardiness assessments; supplies in year 1 include materials to build 'polar pod' system (datalogger, thermocouples, heating elements, power supply) for hardiness evaluation in spring (i.e., when DTA is ineffective)

OBJECTIVES

1. Evaluate the utility of cellulose nanocrystals (CNC) applications for reducing cold damage
2. Summarize and disseminate key findings with stakeholders

SIGNIFICANT FINDINGS

- We have developed a reliable process for creating dispersions of cellulose nanocrystals (CNC)
- CNC treatments via handheld electrostatic sprayer provided resistance to cold damage in apple and sweet cherry
- CNC at 1 % was less effective than CNC at 2 %
- Cold-hardiness could be improved by 0 to 2 F at 1 % CNC treatment and by 3.6 to 7 F from 2 % CNC treatment
- CNC treatment may advance flowering in sweet cherry
- CNC coatings can be 'washed' off during rain
- CNC can be effective up to 7 days post application

Single application results:

Applications made to sweet cherry on 19 March were effective at improving tolerance to cold temperatures. At -2 C and -3 C, 30% of the untreated buds were killed. Nearly 90% of collected buds from the control trees were dead at -5°C, and none of the floral buds survived when temperature reached -7 °C. In contrast, CNC-treated buds were undamaged until -6 °C when pistil mortality was 70%. At the lowest temperature tested, - 9 °C, there were still 10% of CNC-treated buds that survived. A close analysis (Table 1) of mortality data suggested that the LT10 (temperature at which 10% buds are killed) of the control and CNC-treated buds were -1.4 °C and -5.1 °C respectively, whereas the LT90 (lethal temperature at 90% mortality) of the control and treated buds were -5 °C and -8 °C. The LT50 (lethal temperature at 50% mortality) of the control and treated buds were estimated as -4 °C and -5.7 °C.

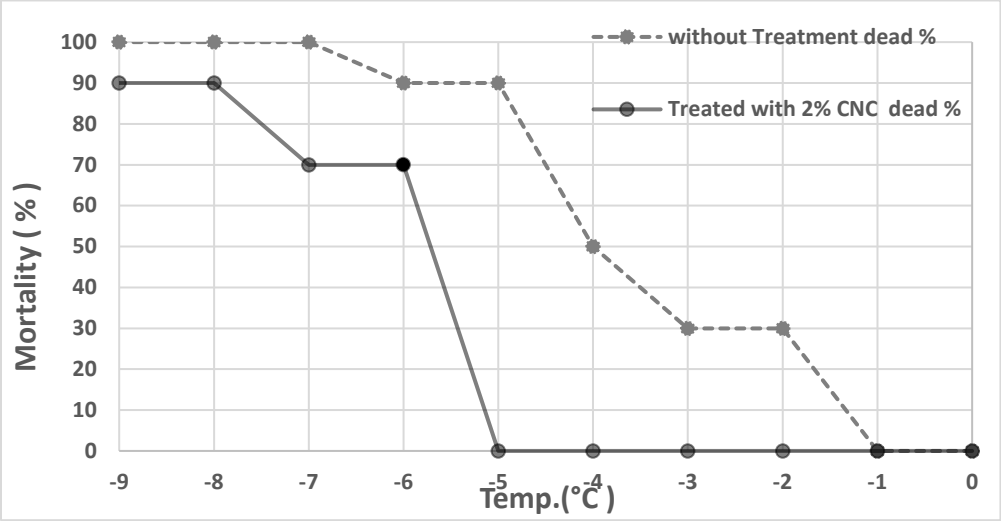

Fig. 1. Mortality of 'Benton' sweet cherry floral buds. Treatment made 19 March. Sampled on 20 March.

The effect of CNC spraying on the hardiness of the buds was determined again on March 26th following the same experimental procedure. Again, the CNC treatment significantly improved the hardiness of buds. Interestingly, untreated cherry floral buds collected in this week exhibited improved cold tolerance in the warmer temperatures evaluated (Fig.). On this sampling date, only 10% of the untreated buds were dead at -4 °C and 60% were dead at -5 °C. Similar to the previous treatment date, -7 °C was a critical temperature at which all reproductive buds were dead. In contrast, the CNC-treated buds exhibited similar sensitivity to cold damage on this date as the previous week. Tissue damage first occurred at -6 °C of CNC-sprayed buds and -9 °C was the critical temperature leading to mortality of all buds.

Based on these two sample dates, spray treatments of 2 wt.% CNC can prevent cold damage in sweet cherry. This is similar to our previous research (Alhamid et al., 2018). We found that all buds treated with CNC were free from damage until – 6 C. In contrast, untreated buds had either 90% or 60% bud death at – 5 C on 19 March and 26 March, respectively. This level of protection from cold damage is potentially significant for commercial growers during early spring frost.

Buds sampled 24 hr after treatment on 2 April exhibited significantly less hardiness, irrespective of treatment (Fig. 8). Untreated control buds exhibited 70% mortality at 0 ºC and complete mortality at -5C. In contrast, CNC-treated buds again were more tolerant to cold temperatures with 0% mortality at 0 C, 70% mortality at -5C, and complete bud death at – 6 C. The LT90 for the control and treated buds were determined at -4.5 ºC and -5.8 ºC. While still effective for improving cold tolerance, the efficacy of CNC treatment at this stage of bud development is less pronounced compared to the results from the previous two weeks.

In the subsequent week, 9 April sweet cherry buds had reached the first bloom stage. At this stage, buds become more susceptible to frost damage. For untreated control buds, we recorded 10% bud mortality at 0 C, with complete death at – 3 C. A temperature drop to -1°C was sufficient to cause 90% mortality of the untreated buds. The CNC treatment again improved bud hardiness, even at this vulnerable stage (Fig. 9). Bud mortality was not observed at 0 or -1 C in treated buds. There was a rapid increase in bud mortality as temperatures dropped, with 20%, 80%, and 100% death at -2, -3, and -4 C. respectively. There was no rain on either April 9th (date of spraying) or April 10th (date of sample collection).

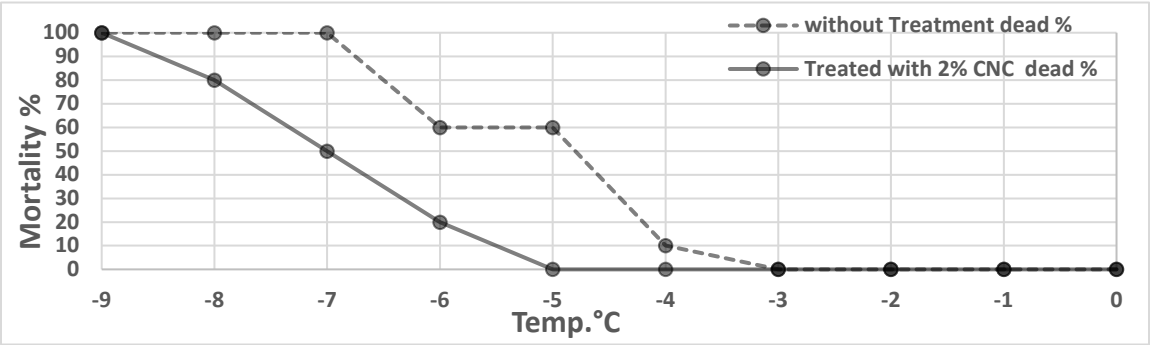

Fig. 2. Mortality of 'Benton' sweet cherry floral buds. Treatment made 26 March. Sampled on 27 March.

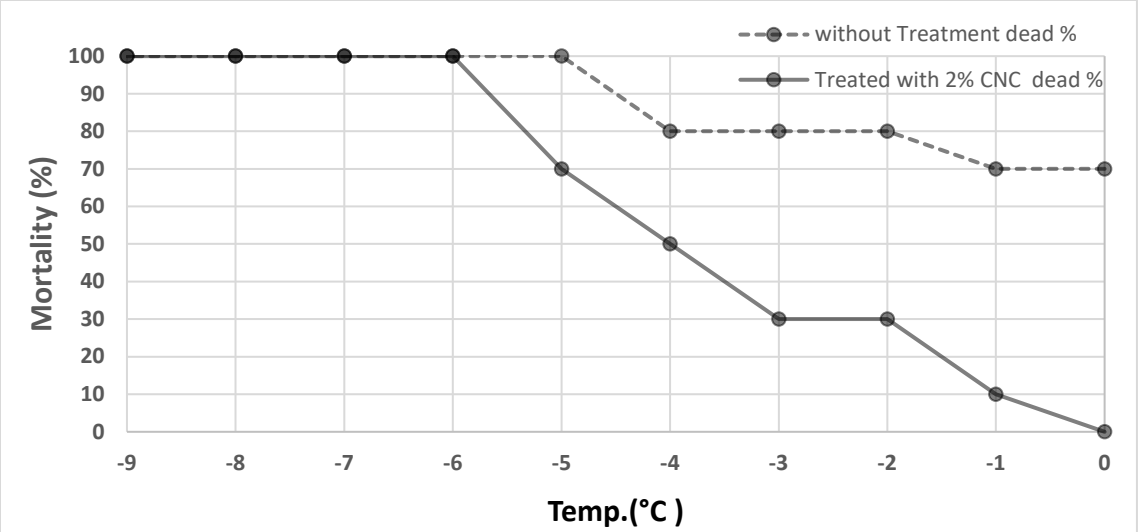

Fig. 3. Mortality of 'Benton' sweet cherry floral buds. Treatment made 2 April. Sampled on 3 April.

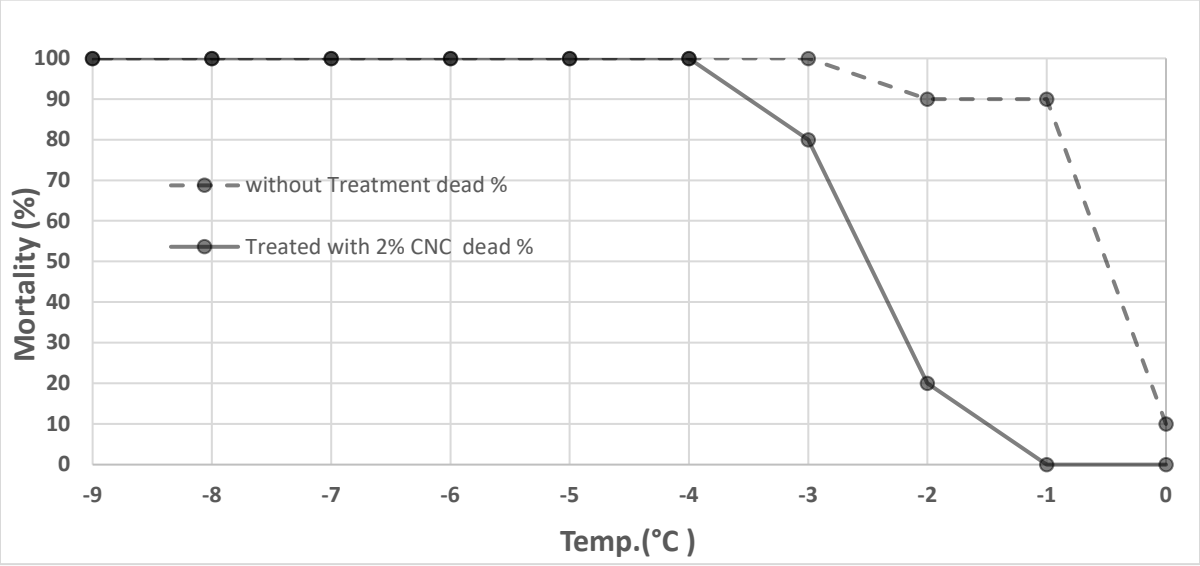

Fig. 4. Mortality of 'Benton' sweet cherry floral buds. Treatment made 9 April. Sampled on 10 April.

Multiple application testing results

All previous trials of CNC in fruit crops have assessed effects of single applications on cold damage. It is important, however, to understand whether repeated applications of CNC may further improve bud hardiness. In this trial we examined cold tolerance of buds that had received multiple applications of CNC. The initial CNC treatment on 19 March improved cold hardiness of buds to a similar degree to the other trial (Fig. 1), confirming the efficacy of single sprays. A second application was made to the same trees on 26 March, and buds collected after 24 hours following the 2nd second spray exhibited hardiness (Fig. 5) that was similar to the single treatment efficacy (Fig. 2). This suggests that a single application of CNC may be adequate for frost protection. Future research in our lab will assess this issue more thoroughly. The lethal temperatures obtained from control and treated buds are shown above, these data generally agree with the single applications testing results (Figs 1-4).

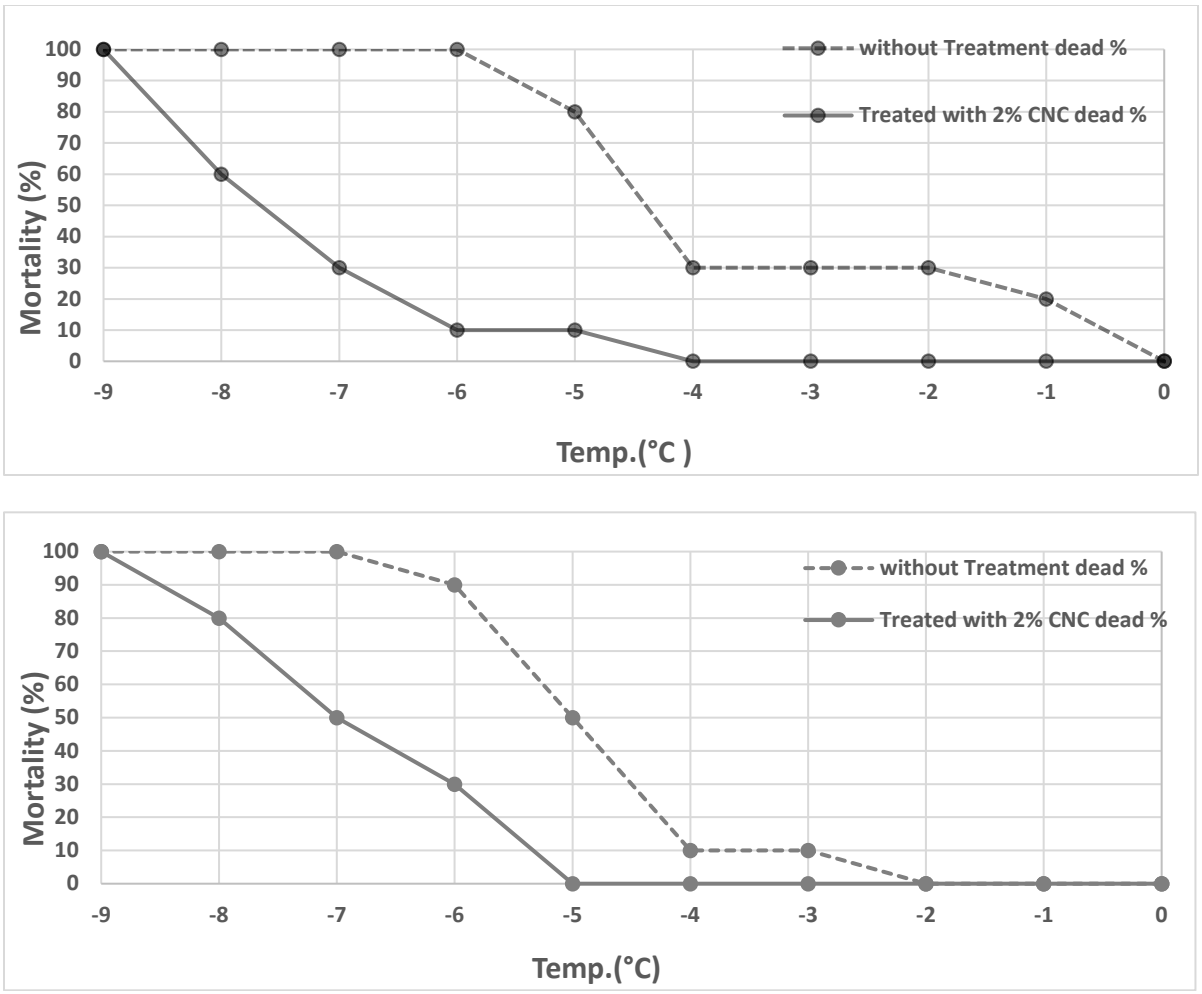

Fig. 5. Mortality of 'Benton' sweet cherry floral buds. Treatments made 19 April and 26 April to same trees. Buds were sampled on 20 April (above plot) and 27 April (lower plot).

Large-scale commercial trial

The results obtained from the field trials conducted at the WSU experimental station have confirmed the earlier results from the laboratory studies (Alhamid et al., 2018). It is clear that CNC treatment is an innovative and effective technology to prevent frost damage to tree fruits. These trials have utilized small-scale application systems that may not represent well the actual efficacy of CNC treatments made on a large scale, with commercial application technologies. To further determine the commercial potential of this technology, large-scale trials were conducted in Spring 2019 at two commercial orchard locations, Mattawa, WA on 20 March 20, and Pasco on 21 March. One acre of sweet cherry and one acre of apple were selected at each location for the trials. During the trial, a commercial sprayer was used (On Target Spray Systems, Mt. Angel, OR, USA; Figure 12). The sprayer had 32 electrostatic nozzles and reservoir tank with a capacity of 100 gallons (378.5 L) (Figure 12a). Results are promising (Figs 6 &7).

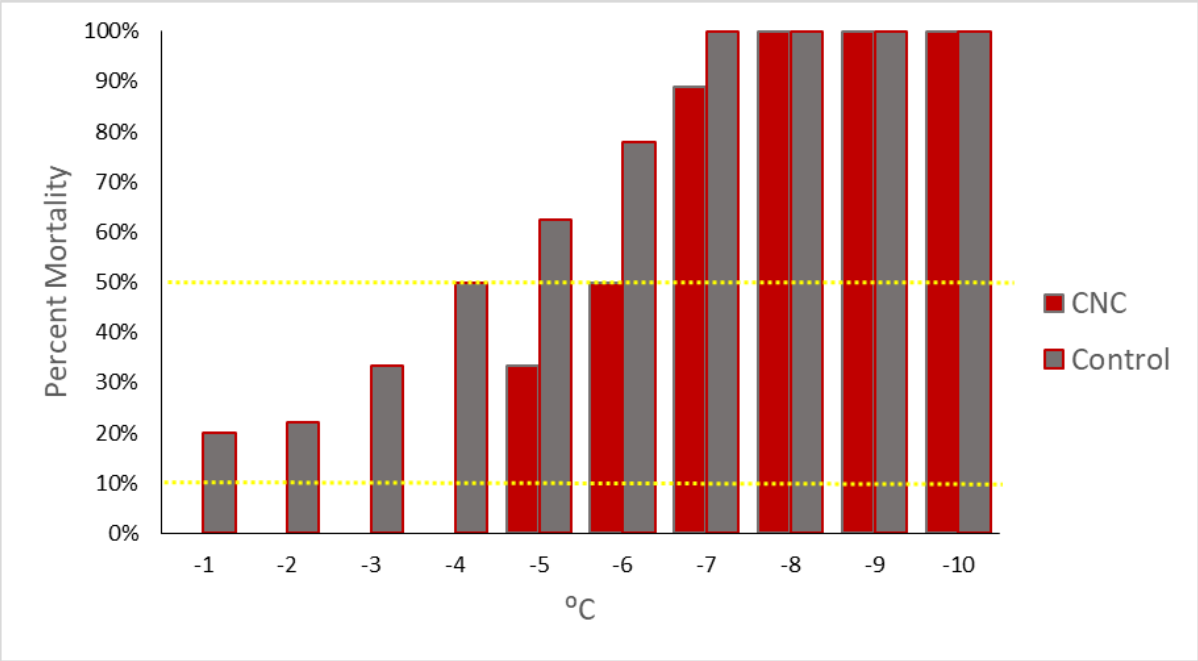

Fig 6. Mortality of 'Benton' sweet cherry buds 6 days following application of 2.5% CNC with commercial application equipment

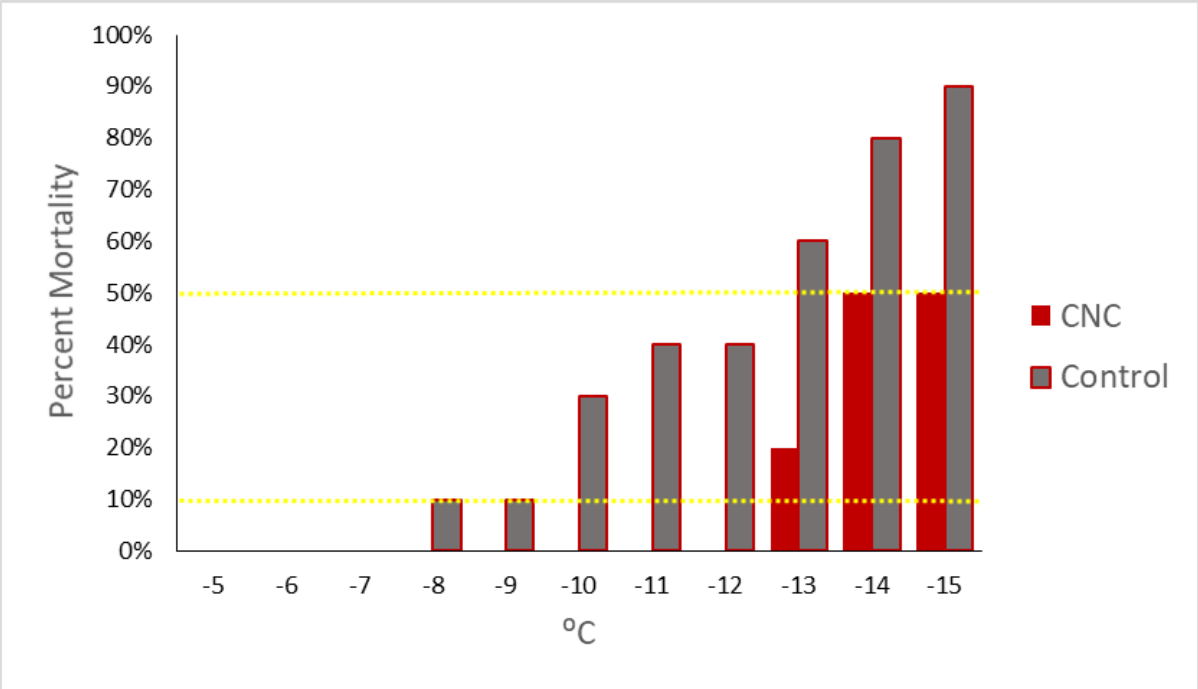

Fig 7. Mortality of 'Gala apple buds 6 days following application of 2.5% CNC with commercial application equipment

EXECUTIVE SUMMARY
Project title: Reducing cold damage with cellulose nanocrystals

Key words: Frost, freezing, CNC, abiotic stress, apple, sweet cherry

Abstract: Applications of cellulose nanocrystal dispersions can reduce cold damage in apple (*Malus domestica* Borkh.) and sweet cherry (*Prunus avium* L.). Reductions in cold damage are related positively to CNC concentration. Protection can last at least 1 week. CNC treatment does not affect flowering time nor fruit set.

Every year, tree fruit growers lose money from cold damage to reproductive buds or flowers. The U.S. Food and Agriculture Organization reported that cold damage has caused more economic losses to crops in the U.S. than any other weather hazard. The potential losses from cold damage are devastating, and predicted to become more commonplace with increasingly variable spring weather. Cellulose nanocrystals (CNC) represents a new generation of renewable nano-biomaterials with unique physical, and chemical properties, including their low thermal conductivity (i.e., they provide excellent insulation). In this work our team has synthesized a CNC dispersion that can be sprayed onto trees, forming a thin, uniform and insulating film on the surface of the buds. The CNC film is transparent, allowing sunlight to penetrate during the day, while its insulating property prevents heat loss during cold conditions.

Single applications of CNC, using electrostatic application technology, can provide significant protection to dormant and post-dormant reproductive buds in apple and sweet cherry. Benefits of CNC treatment are related positively to rate of CNC – 1% CNC provided only slight reductions in cold damage whereas 2% was consistently effective, and 2.5 – 3% provided even greater reductions in cold damage. In 'Scifresh' apple, for example, the LT10 was 30.2 F for untreated flowers and 26.6 for flowers treated with 2% CNC (an improvement of 3.6 F). In this trial the greatest improvement in flower hardiness was observed at 21.2 F, a temperature at which 80% pistil death was recorded for control, 90% for 1% CNC, and only 30% for 2% CNC. Based on these results, untreated trees would have complete crop loss at about 19 – 20 F, and trees treated with 2% CNC would have ca. 50% crop remaining, not losing the entire crop until ca.16 F. Importantly, we discovered that CNC efficacy is not lost in large-scale applications using commercial sprayers (OnTarget Spray Systems). We found that a 2.5% CNC treatment improved hardiness of sweet cherry and apple by

Interestingly, multiple applications of CNC dispersions to trees did not improve tolerance to cold temperatures any more than single applications. This was evaluated however in only a single trial, and this is an area for further research. We have shown that the protection of CNC coatings is lost during rain, but that a single treatment can provide significant improvement in hardiness for up to one week in the absence of precipitation. It is unclear how much precipitation is sufficient to reduce the CNC film's efficacy – this too is an area for further research.

FINAL PROJECT REPORT **YEAR: 3 (of 2+1yr NCE)**
WTFRC Project Number: TR-17-100

Project Title: Enhancing reference genomes for cross-cultivar functional genomics

PI: Loren Honaas
Organization: USDA, ARS
Telephone: (509)664-2280
Email: loren.honaas@ars.usda.gov
Address: 1104 N. Western Ave.
City/State/Zip: Wenatchee, WA 98801

Co-PI: Joshua Der
Organization: Cal State University, Fullerton
Telephone: (657)278-4115
Email: jder@fullerton.edu
Address: 800 North State College Blvd.
City/State/Zip: Fullerton, CA 92831

Cooperators: Stefano Musacchi & Sara Serra (WSU-TFREC), Claude dePamphilis (PennState)

Total Project Request: **Year 1:** $48,832 **Year 2:** $35,207

Percentage time per crop: Apple: 60% Pear: 40% Cherry: NA Stone Fruit: NA

Other funding sources: None

Budget 1
Organization Name: USDA, ARS **Contract Administrator: Chuck Myers**
Telephone: 510-559-5769 **Email address: chuck.myers@ars.usda.gov**

Item	2017	2018
Wages[1]	$12,500	$12,500
Equipment	$3,750	$750
Supplies	$3,000	$3,722
Miscellaneous[2]	$11,664	NA
Total	$30,914	$16,972

Footnotes:
[1]Data analysis including Research Support Agreements to cooperators
[2]Cooperative Agreement for PacBio library prep + sequencing to Penn State Group

Budget 2
Organization Name: CSU Fullerton **Contract Administrator: Alison Nguyen**
Telephone: 657-278-7621 **Email address: allisonnguyen@fullerton.edu**

Item	2017	2018
Salaries[1]	$8,922	$9,234
Benefits[1]	$129	$134
Wages[2]	$8,526	$8,526
Benefits[2]	$341	$341
Total	$17,918	$18,235

Footnotes:
[1]Salary and benefits for Joshua Der – 1 month
[2]Salary and benefits for Der lab student – 2 semesters

OBJECTIVES

Enhance discovery of genetic factors associated with fruit quality differences using existing and in-progress RNA-seq data, along with publicly available genomic resources:

Step 1) **identify genetic differences** between reference genomes and genomes of interest ('Golden Delicious' vs 'Granny Smith' & 'Bartlett' vs. 'D'Anjou').

Step 2) use bioinformatic approaches to **update the reference genomes** to reflect these differences creating custom, polished references for analysis of gene expression in each of the genomes of interest.

Step 3) **compare gene expression results** from the original and polished versions to calculate changes in read mapping rates focusing on total reads matched and changes in uniquely matched reads (both indicating changes in sensitivity for measuring gene activity) **to evaluate the efficacy of the genome polishing strategy.**

SIGNIFICANT FINDINGS

Progress on specific objectives:

- **Step 1) Exceeded -** We identified genetic differences between reference cultivars and cultivars of interest, finding millions of polymorphisms across the whole genome, not just in gene sequences
- **Step 2) Exceeded** - By sequencing the full genome of 'Granny Smith' and 'D'Anjou', we can account for 10s of thousands of gene sequence polymorphisms captured in recent experiments, and we discover virtually all 'Granny Smith' and 'D'Anjou' genes, not just those shared with reference cultivars 'Golden Delicious' and 'Bartlett'
- **Step 3) Exceeded –** We can bring ~10-15% more gene activity data into an analysis by mapping to our cultivar specific genomes than to the reference genomes for 'Golden Delicious' and 'Bartlett'. Additionally we characterized the effect of polymorphisms on specific genes

Other important findings:

- Differences among the genome sequences of *Malus* and *Pyrus* cultivars are problematic for gene activity measurements
- Affected genes may be important for understanding important fruit quality traits
- Apple and pear genomes provide research opportunities beyond gene activity measurements that will help us understand pome fruit traits
- Genomes also facilitate:
  - access to more cost-effective gene activity measurements
  - deeper comparative genomics in apple and European pear
  - access to emerging technologies for gene activity analysis

RESULTS & DISCUSSION

Excerpt from the project proposal justification

Recent technological advances have allowed researchers to measure the activity of all genes in a sample simultaneously using a method called RNA-Seq. This approach uses Second Generation Sequencing to create hundreds of millions of measurements called "reads" – these are the RNA-Seq basic unit of measurement. The reads from each sample are counted with sophisticated software by matching reads to the DNA sequence of known genes. This critical step in analyzing RNA-Seq data relies on existing knowledge of the genes being measured and assumes that the RNA-Seq data perfectly matches the existing genes. These known genes come from sequenced **genomes** – genomes are the collection of all genetic material in an organism, a small fraction (~5%) of which are the genes. A reference genome exists only for one apple cultivar, 'Golden Delicious', and one European pear, 'Bartlett'. However, commercially produced apples and pears contain substantial genetic diversity within and among cultivars. When doing RNA-Seq in other cultivars, these genetic differences (polymorphisms) may present substantial challenges when obtaining gene activity measurements in postharvest fruit quality experiments.

For example, genetic differences between 'Golden Delicious' and 'Granny Smith' may lead to loss of signal in RNA Seq experiments because 'Granny Smith' reads may fail to be assigned to the correct gene (or at all) in the reference 'Golden Delicious' genome, due to a *mismatch* (see Box 1).

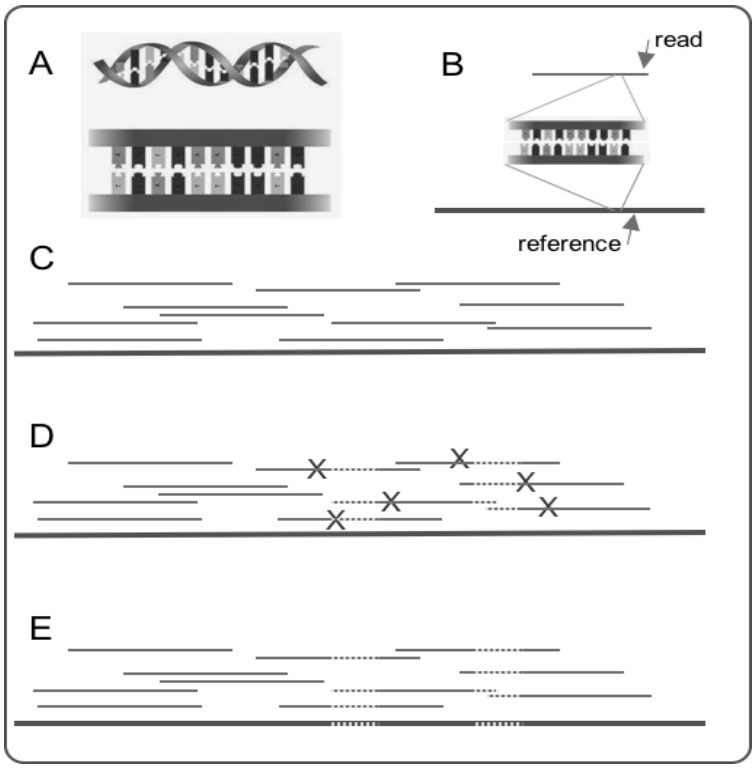

Box 1. RNA-Seq data analysis relies on digitally matching reads, letter-by-letter, to the DNA sequences of genes. A) *rendering of the DNA double helix (top) and flattened version (bottom) more typical for visualizing DNA sequences (image credit -http://biology4alevel.blogspot.com/),* ***B)*** *zoomed schematic showing how reads are matched, letter-by-letter, to reference genes where the position of the read indicates where it matches to the reference,* ***C)*** *'Golden Delicious' example where reads match the reference and are mapped successfully,* ***D)*** *'Granny Smith' hypothetical example where polymorphisms (dashed regions of the reads) fail to map to the correct position,* ***E)*** *example of a polished apple reference corrected for use with 'Granny Smith' that allows reads to map successfully.*

The question that led to this project was straightforward: "What is the effect of genetic mismatches between genomes in RNA-Seq experiments?" This led to the following hypothesis.

> ***If the genes that explain differences in cultivars tend to be different, and if these differences are related to loss of signal in gene activity measurements, then the genes that may explain important cultivar differences are the most likely to be missing from gene activity analyses.***

Simply put, the genes that make 'Granny Smith' fruit different from 'Golden Delicious' fruit may be dropping out of our gene activity experiments because they are genetically different. If those missing genes are involved with important fruit quality traits (like Superficial Scald susceptibility), this creates a critical blind spot when we use genomics tools like RNA-Seq to learn about those important fruit quality traits.

Analogy of the problem

The issue described above can be illustrated in a jigsaw puzzle analogy. The RNA-Seq data units, called reads, can be thought of as jigsaw puzzle pieces. The reference genome is best thought of as the picture that comes printed on the jigsaw puzzle box that can be consulted by the user to guide where to put puzzle pieces. The issue with mismatched genomes is that the puzzle pieces do not perfectly match the picture on the box (Box 2). A skilled user could probably finish the puzzle if it consisted of a few thousand pieces. However, an RNA-Seq puzzle consists of hundreds of millions of pieces, and the picture is ~100 times higher resolution than a 4k Ultra HD television. So, necessarily, sophisticated software on high performance computers are needed to complete the task.

In fact, large portions of the puzzle *can* be put together using software that does not need a reference "picture" – this is how we built gene models early in the project. Yet those pictures were not fully complete due to inherent limitations of the process. Assembling a genome is the only way to get the whole picture.

Box 2. *In the puzzle analogy, when the pieces are assembled correctly, they would create the picture in "A." But when using the picture in "B" to guide assembly of the puzzle, the result would be an incomplete image in portions of the picture where the two were most different.*

Genetic differences between cultivar specific genomes and reference genomes – Step 1

Step 1 was to scan the genomes of 'Granny Smith' and 'D'Anjou' to find differences compared to the reference cultivars 'Golden Delicious' and 'Bartlett,' respectively. We eventually found millions of small differences - Single Nucleotide Polymorphisms (SNPs) and small insertions or deletions (InDels) in 'Granny Smith' apple (5.18 million) and 'D'Anjou' pear (5.60 million) (Figure 1). While many of these differences were located in between genes, some of these differences did occur in the genes themselves (e.g. in one experiment we observed 490,275 polymorphisms across 'Granny Smith' apple genes). This is critically important, because genes, while they only represent about ~5% of the apple and pear genomes, are the target for interpreting gene activity measurements in RNA-Seq experiments. *Malus* and *Pyrus* genomes over all are known to be polymorphic, but the extent to which ***genes*** are polymorphic had not been thoroughly examined, nor had there been a detailed exploration of the effect on gene expression analyses using a genetically mismatched genome reference.

Initially, using our raw 'Granny Smith' gene activity data we built cultivar-specific gene models and searched for matches to known 'Golden Delicious' genes. Then for a small set of genes we explored the effect of polymorphisms by comparing gene activity measurements between a gene-by-gene approach (1 gene at a time - qPCR) vs. the global approach (all ~40,000 genes at once – RNA-Seq). We published a paper (Hargarten et al. 2018 - https://doi.org/10.21273/JASHS04424-18) that included a protocol for improved RNA-Seq data validation, and we also found some evidence that polymorphisms can interfere with RNA-Seq gene activity measurements. However, that was based on a small number of genes, so we proceeded to the next step which was to modify or polish the reference genomes to account for polymorphisms. This would provide a large gene sample size to compare experimental results the reference genomes and the polished versions.

Building a better reference for RNA-Seq – Step 2

The original strategy for Step 2 was to use the raw gene activity data to identify and then modify or polish polymorphisms in the genes of reference cultivar genomes. However, during the first year of the project, advancements in 3rd generation genome sequencing technology reduced the cost of obtaining high-quality genomes. This created the possibility of building new cultivar-specific genomes, instead of just polishing the publicly available reference genomes. This new approach was preferred for several reasons: 1) a full genome contains all the genes, whereas the raw gene activity data from fruit could only be used to polish genes that were active in fruit, 2) a full genome can show us large scale differences (not just SNPs and small InDels) that can help explain cultivar trait differences, 3) the full genome will include genes that are unique to 'Granny Smith' apple and 'D'Anjou' pear, showing us gene content differences that may help explain cultivar trait differences.

We therefore shifted our focus to obtaining data to build 'Granny Smith' and 'D'Anjou' genomes. The price decrease in 3rd generation genome sequencing technology (PacBio) allowed us to access the technology, but not enough to allow us to build a genome solely from long read data. Thus, we generated a hybrid data set consisting ultimately of 4 kinds of genome data; Illumina, PacBio, Oxford Nanopore, and 10x. Except for Illumina, which is a second-generation technology, these 3rd generation technologies take advantage of high molecular weight DNA (very long pieces) in either the sample preparation or the sequencing step. The resulting larger pieces of data effectively reduce the complexity of the genome assembly task. Following the puzzle analogy above (Box 2), this data type creates puzzles with larger pieces that are easier to assemble.

These multiple data types were assembled and postprocessed via a proprietary method that is in development in the dePamphilis lab at Penn State. We predicted based on the volume of data that the assemblies would be at least good enough to recover the complex portions of the genome that included genes. In fact, the genomes are highly complete, with recovery of fragments that account for virtually all of the *Malus* and *Pyrus* chromosomes (Figure 2). Further, when assessing the completeness of complex plant genomes like these, searching for genes that are shared widely across all plants is indicative of completeness. This method is called Benchmarking Universal Single Copy Orthologs (BUSCO) – the BUSCO completeness score for the 'Granny Smith' genome was 96.2% and for

'D'Anjou' was 97.2%. These metrics indicate that the gene content for the cultivar specific genomes are highly complete. This is a substantial increase over the BUSCO scores of ~65% in the gene model collections we initially built from the raw gene activity data in 'D'Anjou.' These results indicate that the 'Granny Smith' and 'D'Anjou' genomes will contain all the genes that are represented in RNA-Seq experiments.

With good genome assemblies in hand, we selected one to test the next step of annotation which involves scanning the ~600 million letters of DNA code (consisting of A,T,G, & C) to find genes, and then identifying them by comparison to known genes. We chose pear because our results suggested that *Pyrus* would benefit more than apple from cultivar specific genomes, and because of synergy with Honaas' pear project (WTFRC Project PR-17-104 "Functional Genomics of 'D'Anjou' Pear Fruit Quality and Maturity") that had a substantial RNA-Seq component that would likely benefit from the 'D'Anjou' genome v1.0. Briefly, the annotation process involves using the gene models we built from the raw 'D'Anjou' gene activity data in the initial phases of the project, combined with all the available resources for pear genes at the Genome Database for Rosaceae (https://www.rosaceae.org/). Luckily, this included 3 new pear genomes made public in 2019 - *Pyrus betulifolia* v1.0*, Pyrus ussuriensis* x *communis* v1.0*,* and *Pyrus communis* 'Bartlett' v2.0 (https://www.rosaceae.org/). The annotation results were concordant with results from the published Bartlett genomes v1.0 (Table 1), further indication of the high quality of the 'D'Anjou' genome v1.0. With updated RNA-Seq references and a catalog of differences between the cultivar-specific genomes and reference genomes, we moved on to Step 3.

Polymorphisms between pome fruit genomes interfere with RNA-Seq data measurements – Step 3A

As stated above, we had data from a small number of genes that suggested polymorphisms might be interfering with RNA-Seq based gene activity measurements. Concurrent with the effort to sequence and assemble the genomes of 'Granny Smith' and 'D'Anjou,' we developed a bioinformatics test that would help reveal the effects of polymorphisms on RNA-Seq measurements. Counterintuitively, this involved making the RNA-Seq reads even smaller. The idea was that if a 'Granny Smith' RNA-Seq read matched to a 'Golden Delicious' gene but had enough small differences that the computer program could not confidently match it, then by fragmenting the reads we might be able to separate out the pieces that matched perfectly from the ones that contained differences. Then the parts that matched perfectly would be successfully assigned, causing a recovery of the gene activity signal. We ran this test using a subset of RNA-Seq data from our published 'Granny Smith' work (Honaas et al. 2019 - https://doi.org/10.1016/j.postharvbio.2018.09.016).

We found that genes that contained differences showed a recovery in gene activity signals, and that the signal recovery was flanked by known genetic differences between 'Granny Smith' and 'Golden Delicious' (Figure 3A). Unfortunately, this test is not a solution to our problem. This is because while fragmentation of the reads helps recover the gene activity signal for genes with differences, for other genes the signal becomes ambiguous and therefore reduced (Figure 3B). We then examined the pattern across all genes for multiple samples, finding that there is a significant positive correlation (R^2=0.36±0.02, p=2.2e-16) between recovery of signal and polymorphisms when mapping fragmented reads (Figure 3C).

With further development this test may be useful to estimate the extent to which gene activity measurements are affected by genetic mismatches, especially with regard to tuning the parameters during the step where reads are matched to genes. For our purposes, it illustrates that there are pitfalls associated with mapping RNA-Seq data across cultivars. These pitfalls can be potentially avoided by providing a closer match between the gene activity data and the reference genome.

RNA-Seq mapping improves in a genetically matched genome – Step 3B

The final tests involve examining how the genomes perform as references for RNA-Seq experiments. These tests are straight forward, and our predictions about the increases in the proportion of RNA-Seq read data that could be brought into an experiment (15%) were surprisingly accurate. In the initial

annotation tests, we simply lifted over the gene location and structure information from the reference genomes to the new cultivar-specific genomes. This quick and dirty approach allowed us to annotate about 80% of the genes in the new genome. Starting with the apple genes that we examined in the fragmented read test above, we searched the new 'Granny Smith' genome to see if any of those genes were annotated. We did not find many genes that met this citeria, which is expected – the genes that saw signal recovery are among the most polymorphic in fragmented read analysis, and gene differences would cause the lift-over annotation strategy to fail. In Figure 4 there is an example of a gene that was different enough to show a signal recovery in the fragmented read experiment, but not too different such that it was excluded from the fast, reference lift-over annotation. When we mapped the 'Granny Smith' gene activity data at high stringency to both the 'Golden Delicious' genome and 'Granny Smith' genome, we saw the signal in the 'Granny Smith' genome increase. This result indicated that for at least some genes, a matched genome would allow signal recovery compared to a mismatched genome when used for RNA-Seq.

The last test was to run a full RNA-Seq experiment with the new fully annotated 'D'Anjou' genome. We ran the analysis 3 times with identical parameters: once with the 'Bartlett' v1.0 genome, once with the recently released 'Bartlett' v2.0 genome, and last with our 'D'Anjou' genome v1.0 (Figure 5). This test shows us that we can assign more RNA-Seq data to pear genes when we used a genetically matched reference genome. Furthermore, we observed that the mismatch rate, deletion rate and insertion rate were roughly twice as high when mapping to the 'Bartlett v2.0' genome, indicating that we could increase the stringency of the mapping parameters and enhance the confidence of our gene activity results when using the 'D'Anjou' genome.

Perspectives

The hypothesis that led to the proposal for this work started with the question "What is the effect of genetic mismatches between genomes in RNA-Seq experiments?" The answer we now have is that a genetically matched genome reference is better for RNA-Seq because we bring more data into the analysis at higher stringency, giving us an overall increase in the confidence of our gene activity measurements, leading to higher confidence in the biological stories these data tell.

By opting to sequence and assemble the whole genomes of 'Granny Smith' and 'D'Anjou' pear, we substantially increased our genomics tool kit for apple and European pear. It is important to note that these genomes are not endpoints but starting points for comparative genomics in these species. These are called draft genomes because they are works in progress. The area that needs the most improvement is the annotation of the genomes. This is a complex and iterative process, yet the first pass annotation showed us that there may be genes in the 'D'Anjou genome that are missing from 'Bartlett' versions 1 and 2. If this is proven to be the case, these genes would be totally absent from an 'D'Anjou' experiment using either of the 'Bartlett' genomes. The genomes also provide opportunities to leverage higher efficiency RNA-Seq data types that target small portions of genes, but which require the cultivar specific genomes we now have. We can now potentially access cutting edge data analysis tools, like Salmon (https://combine-lab.github.io/salmon/) which are super-efficient, yet require very high accuracy gene models which we now have with the 'Granny Smith' and 'D'Anjou genomes. Last, we can now more easily identify genes that are most different between 'Bartlett' and 'D'Anjou' providing exciting new opportunities to discover the genetic basis of the differences between these cultivars.

FIGURES AND TABLES

Figure 1. Cultivar specific genes are polymorphic.
A) An example of a **polymorphic** 'Granny Smith' gene showing both Single Nucleotide Polymorphisms (SNPs) and an Insertion/Deletion (InDel).
B) CIRCOS plots summarize a scan of 'Granny Smith' apple and
C) 'D'Anjou' pear genomes showing polymorphisms (outer trace) and genome data coverage (inner trace). Each block represents a large genomic fragment and the entire genomes of apple and pear are represented.

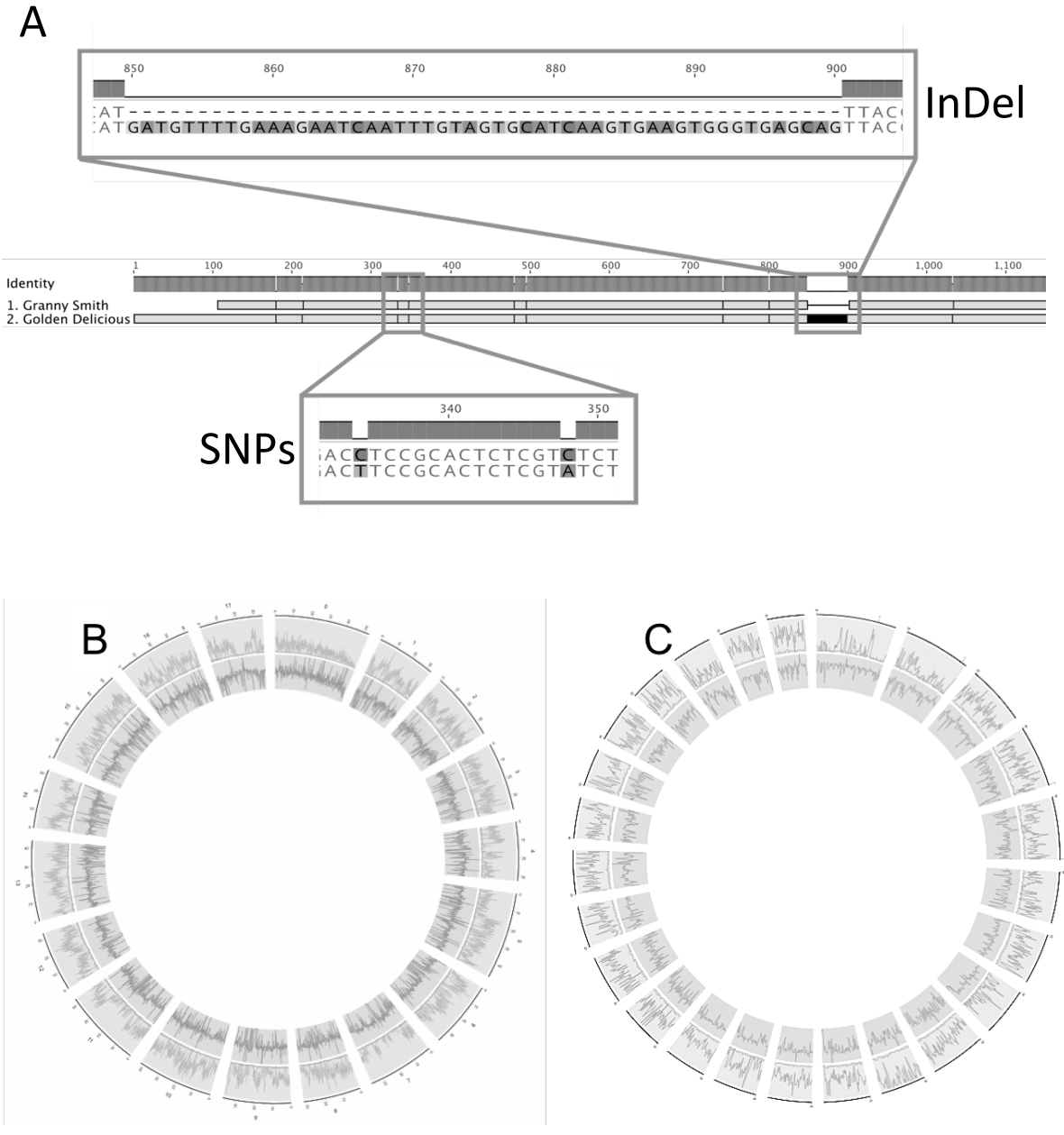

Figure 2. The *Malus* and *Pyrus* genomes we sequenced for this project are highly complete.
A) 'Granny Smith' and 'B) 'D'Anjou,' were lined up against the known reference genomes to estimate completeness. A straight and unbroken line from the lower left corner to the upper right corner indicates that for every portion of the reference genome, there is a corresponding piece of the cultivar specific genome that is in the correct orientation.

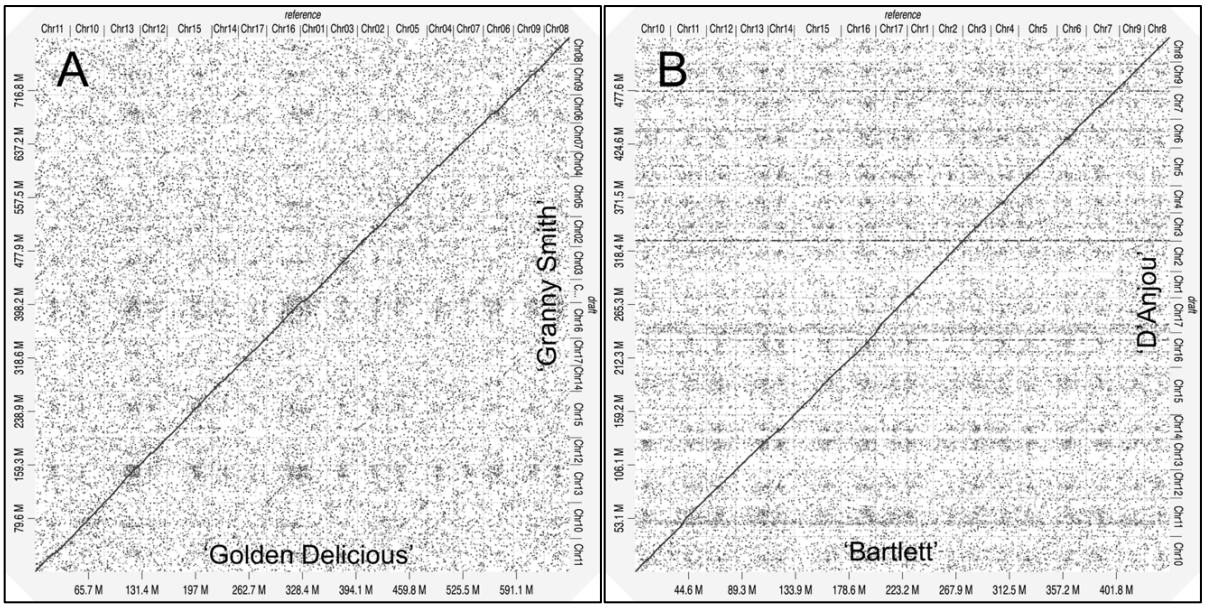

Figure 3. Polymorphisms can prevent reads from being matched to a reference gene. In panel A, Fragmented 'Granny Smith' reads match to the reference gene in between polymorphisms (arrow heads) that prevented the full length reads from matching to the reference gene. In panel B, signal is lost for a different gene when the reads are fragmented because the match becomes ambiguous – the reads match multiple similar genes in the 'Golden Delicious' genome. In panel C the pattern across all genes detected in the experiment shows that the number of differences (e.g. polymorphisms) is proportional to signal recovery in the fragmented read experiment. The genes that were most different showed the highest signal recovery when we matched read fragments in between polymorphisms.

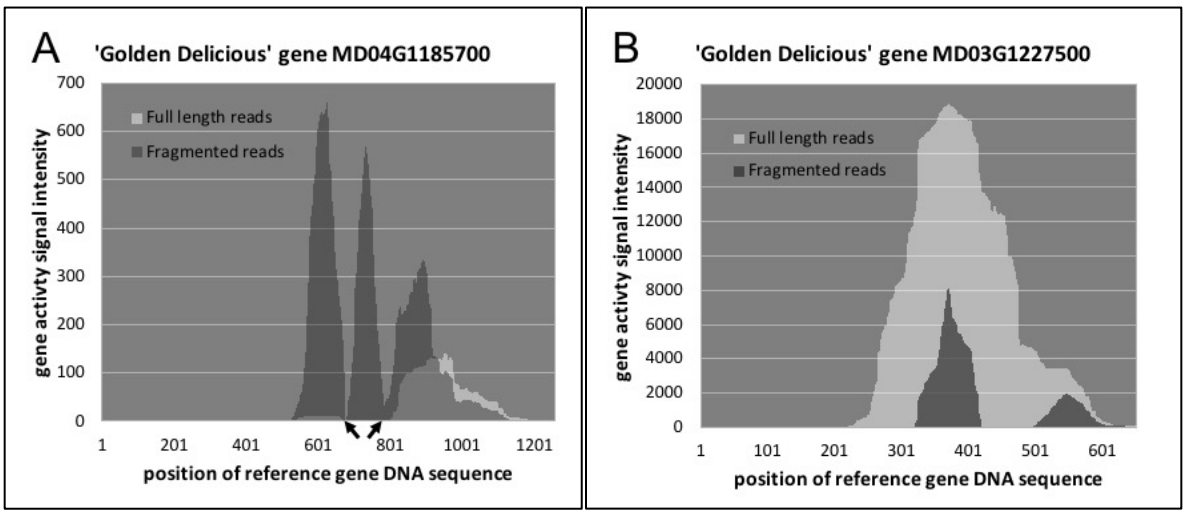

Figure 3C.

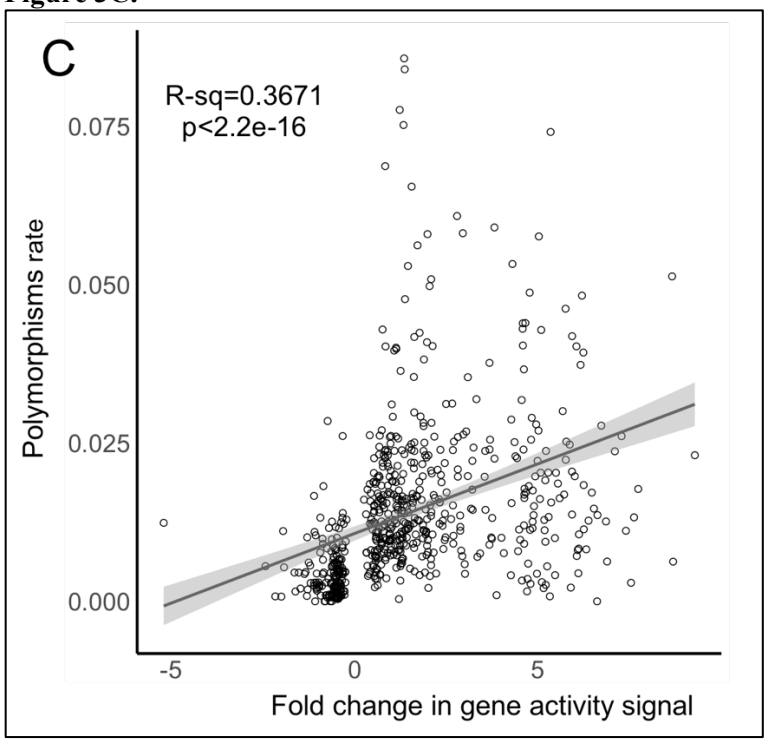

Figure 4. RNA-Seq signal recovery between to different experiments shows the same pattern. When we changed the structure of the read data to fit in between polymorphisms, we saw RNA-Seq signal recovery. In a different experiment, we mapped 'Granny Smith' RNA-Seq data to a partially annotated 'Granny Smith' genome as well as the 'Golden Delicious' genome. For this same gene, we saw a similar signal recovery when using the matched genome. This suggests that genetic polymorphisms can attenuate RNA-Seq signals.

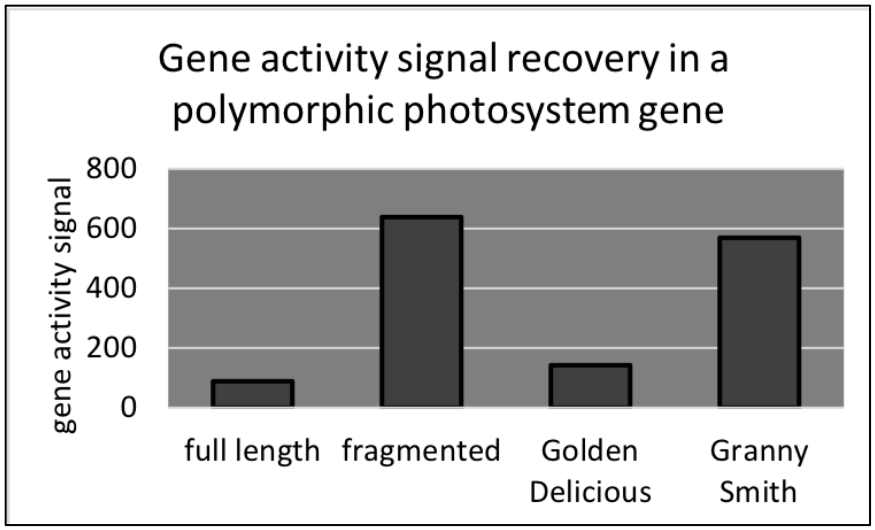

Figure 5. RNA-Seq data mapping was highest when the experimental data and genome matched. This result supports the hypothesis that genetic polymorphisms can create artifacts in RNA-Seq data, that include loss of signal. A matched genome can correct some of these artifacts.

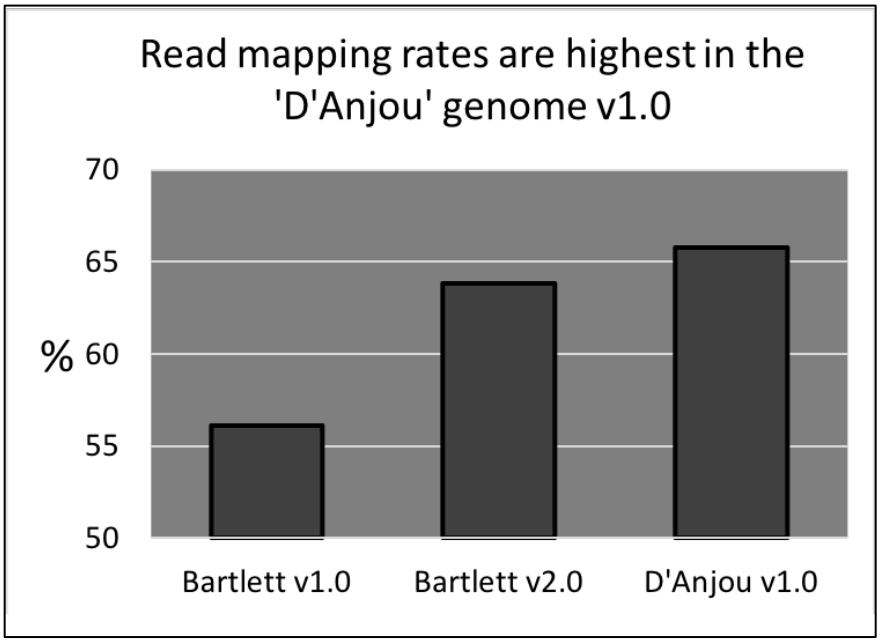

Table 1. Annotation summary for *Pyrus communis* genomes.

	Bartlett v1.0	Bartlett v2.0	D'Anjou v1.0
Number of genes	45,217	37,445	45,981
Number of genes in known plant gene families	34,444	28,547	36,976
% Genes in known plant gene families	76.2%	76.2%	80.4%
% Gene families detected	93.7%	81%	90.7%
Number of unassigned genes	10,773	8,898	9,005
% Unassigned genes	23.8%	23.8%	19.6%
Number of unique plant gene families	5	13	14
Number of genes in unique plant gene families	16	73	43

EXECUTIVE SUMMARY

Project title: Enhancing reference genomes for cross-cultivar functional genomics

Key words: Postharvest, genome, RNA-Seq, biomarker, gene expression, polymorphism, apple, pear

Abstract: The genomes among apple and pear cultivars differ, and these differences likely impact gene activity measurements. We explored methods to account for these differences, finding that cost effective genomes are a viable strategy. The new cultivar-specific reference genomes are a valuable part of efforts to characterize fruit quality traits using function genomics.

Summary: In the age of plant genomics, there are rapidly expanding opportunities to understand important plant traits. Researchers can associate genes with plant traits by scanning for gene activity signatures in experiments that highlight important plant traits. These experiments can improve our understanding of plant gene function, leading to a deeper understanding of plant traits. For instance, a better understanding of pome fruit traits may help us refine and/or develop technology to minimize postharvest losses.

Such experiments can efficiently target genes that are active in a sample. Combined with high performance sequencing machines that can generate 100s of millions of measurements, this approach can measure the activity of practically ***all*** of the ~40,000 apple (or pear genes) in a single experiment. However, like putting together a jigsaw puzzle, the researcher needs an accurate reference picture to know where to put each piece. This problem becomes enormous when trying to assemble a super high-resolution picture from a puzzle with hundreds of millions of pieces. Necessarily, researchers use cutting edge software on high performance computers to automate the task. This puzzle assembly step assumes a near perfect match between the picture and the puzzle pieces. If there are places where the puzzle doesn't match the picture, this can result in incomplete puzzle assembly. **Thus, this project aimed to understand the impact of the genetic differences between the reference genome data from the sequenced cultivars ('Golden Delicious' apple and 'Bartlett' pear) and the cultivars used in our experiments.** While the automated puzzle assembly step can be tuned to account for some small differences, we hypothesized that differences in specific genomic regions can cause the gene activity "picture" to be incomplete – the signal for certain genes would be repressed or lost. Simply, the genes that were the most different might be more likely to drop out of the analysis. Because the trait differences between cultivars are directly related to the genetic differences between cultivars, this could create a critical blind spot for polymorphic genes that help explain the unique fruit quality traits of a given cultivar.

Our results indicate that genetic differences do impact gene activity measurements, and that genes with more differences are more likely to be negatively affected. We explored ways to account for these differences, ultimately settling on genome sequencing due to rapid advances in the field of plant genomics during this project. This approach improved our ability to create a complete gene activity "picture," which now includes more of the highly distinct genes that may explain important cultivar trait differences. Our project initially focused narrowly on improving our ability to detect versions of genes that were still shared between apple and pear cultivars. With full genomes, we can discover additional large scale-genetic differences that can help us understand plant traits. This includes the discovery of genes that are unique to one cultivar or another.

The important investment in cultivar specific genomes allows us to get better gene activity measurements (for less money) and provides a foundational resource for functional genomics in pome fruit. This project has helped pave the way to obtaining this valuable resource for all the cultivars important in the Washington tree fruit market.

CONTINUING PROJECT REPORT **YEAR**: No-Cost Extension

Project Title: Development of economical wifi-connected open-source sap flux probes

PI: Stephen Good
Organization: Oregon State University
Telephone (541) 737-2118
Email: Stephen.good@oregonstate.edu
Address: 200 Gilmore Hall
Address 2: Oregon State University
City/State/Zip: Corvallis, OR 97331

Co-PI (2): Chet Udell
Organization: Oregon State University
Telephone: (541) 737-4043
Email: udellc@oregonstate.edu
Address: 234 Gilmore Annex
Address 2: Oregon State University
City/State/Zip: Corvallis, OR 9733

Co-PI(3): Nik Wiman
Organization: Oregon State University
Telephone: (541) 737-3479
Email: nik.wiman@oregonstate.edu
Address: 4109 ALS Building
Address 2: Oregon State University
City/State/Zip: Corvallis, OR 97331

Cooperators: Oregon State University Experimental Stations, grower cooperators

Total Project Request: $86,320 **Year 1:** $42,723 **Year 2:** $43,597 **Year 3: 0**

Percentage time per crop: Apple: 25% Pear: 25% Cherry: 25% Stone Fruit: 25%
(Whole % only)

Other funding sources: **None**

WTFRC Budget: **None**

Budget 1
Organization Name: Oregon State University **Contract Administrator:** Russel Karow
Telephone: (541) 737-4066 **Email address:** russell.s.karow@oregonstate.edu

Item	2018	2019	2020
Salaries	$26,745	$27,379	
Benefits	$5,978	$6,218	
Wages			
Benefits			
Equipment			
Supplies	$7,500	$7,500	
Travel	$2,500	$2,500	
Miscellaneous			
Plot Fees			
Total	$42,723	$43,597	$0

DEVELOPMENT OF ECONOMICAL WIFI-CONNECTED OPEN-SOURCE SAP FLUX PROBES

Stephen Good[(1)], Chet Udell[(1)], & Nik Wiman[(2)]
(1) Department of Biological & Ecological Engineering, Oregon State University
(2) Department of Horticulture, Oregon State University

Objectives

Statement of Project Objectives:

This project consists of three objectives:

(1) Develop low-cost alternatives to commercially available sap-flux monitoring systems. These probes will be based on published designs recently made available in academic/research literature that are not accessible to typical tree fruit producers.

(2) Develop wireless connectivity protocols that will allow these new sap-flux probes to be monitored remotely via the world-wide web. Measurements will be converted to tree and orchard level evapotranspiration measurements and placed online for end users.

(3) Make available, as extension publications and online, both the probe design and wi-fi connectivity protocols in a format where users with little technical experience can construct/create their own networks with minimal effort.

Overall Relevance for Pacific Northwest Tree Fruit Producers

This project directly addresses a number of key priorities for technology development in the WTFRC Technology Roadmap. The above objectives are designed in a manner so as to be directly beneficial to tree fruit growers in the Pacific Northwest.

It is expected that the direct, accurate, and low-cost monitoring of orchard-level water use obtained through this project will allow growers to reduce production costs while ensuring premium quality fruit is grown for the consumer. This is because accurate water use monitoring will allow for precision application of required water at the orchard block or individual tree level. Effectively, growers will be able to adjust irrigation rates to achieve desired transpiration rates.

Furthermore, accurate water use monitoring will allow for direct surveillance of orchard blocks, and fruit trees that are in danger of drought damage can be identified remotely. When individual or stand transpiration rates fall below critical thresholds, this signals that trees in these locations are not growing properly and should be investigated in person.

Finally, because transpiration, as directly measured in the sap flux probes, occurs only when leaf stomata are open during photosynthesis, transpiration rates can be related to biomass accumulation via photosynthesis. Sap flux measurements can be integrated as the growing season progresses to provide estimates of how much carbon has been assimilated by each individual tree or stand. These can then be translated into yield information about end of season harvest.

Project Activities and Anticipated Accomplishments

During the upcoming year the following activities are planned:

- Increase the precision of our temperature measurements by testing different amplifiers and analog-to-digital converters. This will allow us to turn down the heater which will save power and reduce our impacts on the tree.
- Validate our probes absolute measurements of water use by comparison with measurements from weighing lysimeters (in progress now) and in the field on a set of fruit trees at the North Willamette Extension Station.
- Design a single unified printed circuit board to integrate all the induvial components of housed within the datalogger/transmitter/power supply.
- Implement Long Range (LoRa) wireless communication to an ethernet-connected base station.

Project Schedule for 2019-2020

This project is proceeding slightly behind schedule, and we will require a No Cost Extension to finish this project. The planned activates for the second year of this project are:

REMAINING PROJECT TASKS	**WINTER 2020**	**SPRING 2020**	**SUMMER 2020**	**FALL 2020**
Lab based test(s) of sap flux through a living tree with weighing lysimeter.	■			
Finalize design of sap flux probes for field deployment	■			
Field deployment of sap flux probes in fruit orchards		■		
Refine data transfer and storage protocols		■		
Develop sap flux probe web-based interface for data display		■		
Disseminate project results via extension & journal publications		■	■	■

Significant Findings

During the past year of this project we have made considerable advances:

- We are now using a different sap flux measurement data processing method: the Heat Ratio Method (HRM). The HRM can detect lower sap flow and does not rely on diurnal cycle variations. It also has the potential for lower power consumption. However, this approach requires 3 different physical objects to be inserted into a tree instead of the 2 required for the older Thermal Dissipation Probe (TDP) approach.

- We have modified the probe design to be more robust, using a flexible printed circuit board (PCB) attached to steel rods for strength. The probe only requires three 2mm diameter holes in the trunk. This is shown in Figure 1.

- We are now comparing the calculated sap flows measured with our probe to transpiration losses with a weighing lysimeter. This gives us highly accurate absolute estimates of sap flux against which we can compare our measurements.

- We have designed a durable, waterproof, stake-mountable enclosure (Figure 2).

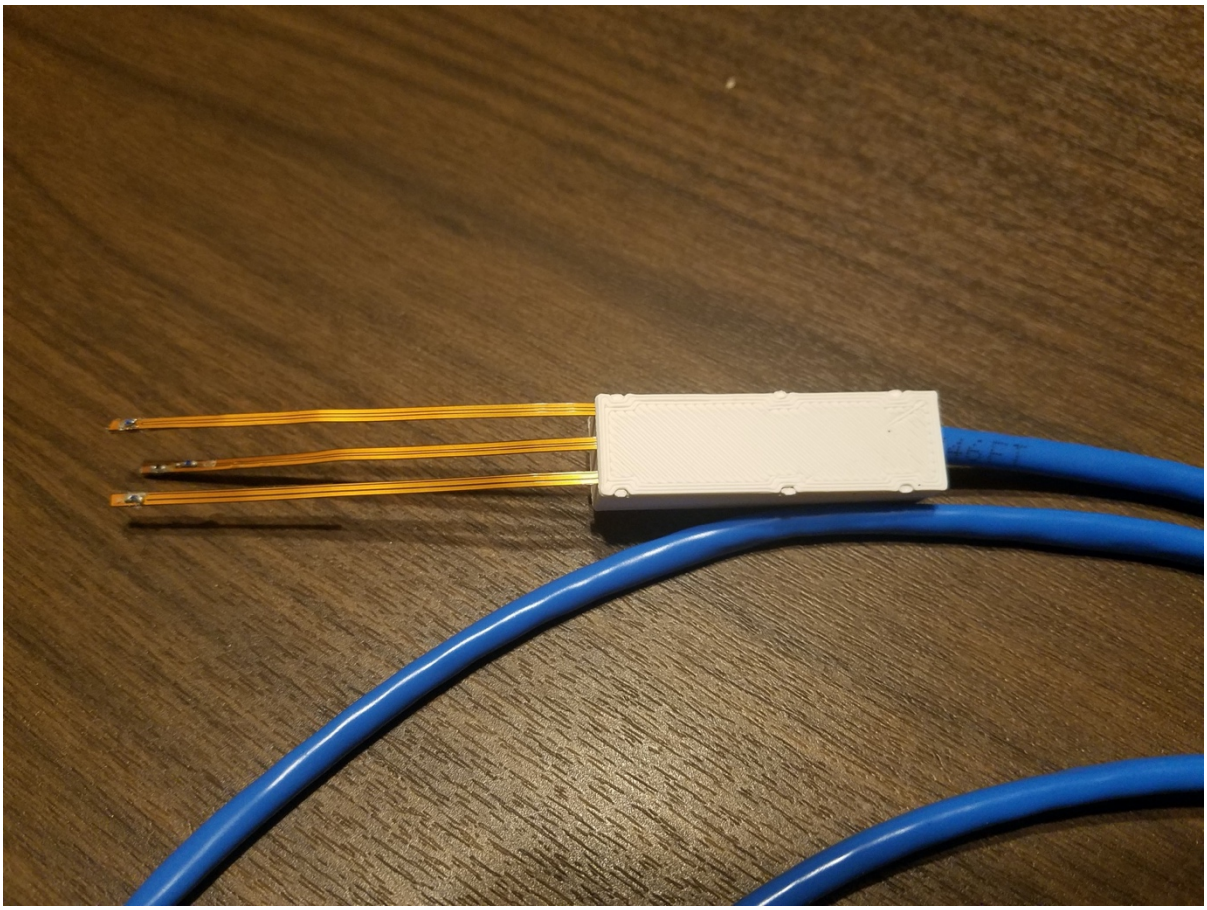

Figure 1: Current version of our HRM probe on the custom printed flexible PCB. Note, the flexible PCB is installed into the tree using rigid guide wire (not shown here).

Methods

This project is focused on development and testing of an economical system to measure sap flow in fruit trees. Our current design uses a flexible printed circuit board (PCB) based approach. The flexible PCB design is shown in Figure 1, and these are inserted into a tree using a rigid metal wire (not shown). These are an improvement over rigid PCB's because they require a smaller hole to be drilled into the tree. Furthermore, by being flexible, they can be inserted at the appropriate depth and then any extra length of the probe that is remains outside the tree can be bent around the stem, thus a single design can work for many sized stems. In total the three-prong probe is expected to cost around $20 itself. This is then connected to to the datalogger and power source using an ethernet cable.

Within the watertight enclosure is a small power source, an Adafruit Feather microcontroller, and a LoRa transmitter, other key electronics such as the heater relay, analog signal amplifiers and an analog to digital converter. A 16GB SD card is also included within this system to store measurements from the HRM probe. Many of these, as well as a few additional components, will all be integrated into a single standard ridged PCB. This system the communicates with a base station using long range (LoRa) wireless radio communication technology. The base station includes an ethernet connection, thus moving observations from the tree to the world wide web, where data can be stored and manipulated as needed. All these components are diagramed out in Figure 3. In total the system is expected to cost about $200 for a single probe, a single datalogger, and a single base station.

Figure 2: Waterproof enclosure with LoRa antenna.

This configuration is fairly flexible, and the datalogger/transmitter is configurable so that

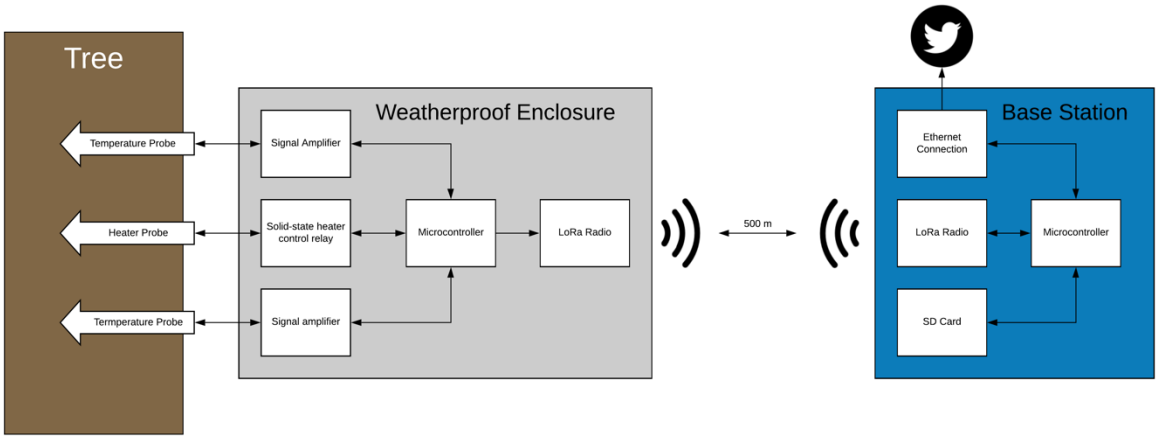

Figure 3: Schematic of the entire system for monitoring tree water use.

multiple probes could be connected to it. The upper limit given the current component selections is 5 probes per datalogger. The limit of how many dataloggers can communicate with the base station is much higher (likely around 100), and the main limitation here is the estimated LoRa range of ¼ mile.

Currently, we are testing this system indoors with a weighing lysimeter. This consists of a small tree placed on a scale. The soil of the pot in which our tree is places is covered with plastic, so the only water lost from is due to leaf transpiration. We are monitoring tree transpiration both with our probe setup and directly by recording the scale weight at regular intervals. This testing began in December and is ongoing now. As a result of this test we will have an accurate assessment of how accurately our probe can measure the absolute sap flux. Following leaf out in spring, we will move our probe system outdoors to test on multiple trees at the North Willamette Research Station. During these tests we will compare our probes with the commercial Dynamax system as depicted in Figure 4

Figure 4: Deployment of our probe (on right) with a Dynamax probe (on left) in a Cherry tree on the campus of Oregon State Universitv 2019.

Results and Discussion

Current System Challenges

Our approach to measurement of sap flux is based on the Heat Ratio Method (HRM). This method is considered to be more accurate than the Thermal Dissipation Probe (TDP). HRM requires less empirical calibration to specific induvial trees then TDP, but also require accurate measurements of temperature ratios. A major limit to this method has been the selection of the correct analog signal amplifier. Our results from testing in 2019 found that the previous amplifier we were employing was not sensitive enough. We have been working on improving this by test out different amplifier and analog to digital signal converters (ADCs). As a result of this the originally chosen Adafruit RTD amplifier has been replaced with a Texas Instruments INA125 instrumentation amplifier, though a newly available integrated amplifier and ADC (Nuvoton Technologies, ~$1.80) is demonstrating promising results.. This transition is expected to significantly improve our measurements; however, the thermal response of this new component needs to be evaluated for linearity. This test is ongoing throughout January 2020. We expect this to be the last major component change for our system. Further modifications are not expected to require changes in hardware selections.

End Of Project Goals:

It is expected that in the upcoming months we will establish a viable, cost-effective, and easily constructed sap flow sensor. We expect that sap flux probes will provide a much better representation of actual orchard-level ET compared to ET estimates calculated from climatological data at remote weather stations. Data from the probes will improve irrigation programs and will lead to greater orchard productivity and may also promote water conservation.

We expect to publish the documentation of the build and programing details in an open access journal such as *Hardware X* (https://www.journals.elsevier.com/hardwarex). This will allow others to take our developed designs and either use time directly or further develop these sensors for their own use. This publication is expected to be completed in Spring and Summer of 2020 is intend to include a comparison of our probes with a commercially available version such as the Dynamax probes. While we do not expect to beat these probes in total performance, we hope to provide reasonable estimates along with a variety of Internet-enabled communications capabilities at a fraction of the price. Finally, in Fall of 2020 we hope to summarize this technical document in a more approachable extension publication that provides information and best practices to the construction, installation, and operation of our sap flow probes.

CONTINUING PROJECT REPORT **YEAR**: 3 of 3 (No Cost Extension)

Project Title: Developing and validating models for tree fruit

PI: Vincent Jones
Organization: WSU-TFREC
Telephone: 509-663-8181x291
Email: vpjones@wsu.edu
Address: 1100 N. Western Ave
City/State/Zip: Wenatchee, WA 98801

Co-PI: Matt Jones
Organization: WSU-TFREC
Telephone: 509-663-8181x290
Email: uchambers@wsu.edu
Address: 1100 N. Western Ave
City/State/Zip: Wenatchee, WA 98801

Co-PI: Tory Schmidt
Organization: WTFRC
Telephone: 665-8271 x4
Email: tory@treefruitresearch.com
Address: 1719 Springwater
City/State/Zip: Wenatchee, WA 98801

Cooperators: None

Total Project Request: Year 1: $90,878 **Year 2:** $94,832 **Year 3:** $99,695

Percentage time per crop: Apple: 40% Pear: 50% Cherry: 10% Stone Fruit: 0%

Other funding sources

Agency Name: WSU Extension
Amt. awarded: $ 198,268
Notes: This is the funding WSU Extension has committed to support maintenance of WSU DAS and implementation of new models.

WTFRC Collaborative expenses:

Item	2017	2018	2019	**2020**
Salaries	6,000	4,000	4,000	**0**
Benefits	2,000	1,200	1,200	**0**
Wages/Benefits[1]	14,000	18,000	20,000	**0**
Supplies	0	0	0	**0**
Travel[2]	2,500	2,600	2,700	**0**
Miscellaneous	0	0	0	**0**
Total	24,500	25,800	27,900	**0**

Footnotes:
[1] Wages/benefits adjusted in years 2 and 3 to reflect new WA minimum wage schedule.
[2] In-state travel to research plots.

Budget 1
Organization: WSU-TFREC **Contract Administrator:** Katy Roberts/Shelli Thompkins
Telephone: 509-335-2885/509-293-8803 **Email:** katy.roberts@wsu.edu /shelli.tompkins@wsu.edu

Item	2017	2018	2019	2020
Salaries[1]	34,020	35,380	36,796	**0**
Benefits[2]	13,442	13,979	14,539	**0**
Wages[3]	8,000	8,320	8,653	**0**
Benefits[4]	216	225	234	**0**
Equipment	0	0	0	**0**
Supplies[5]	2,500	2,600	2,704	**0**
Travel[6]	4,000	4,160	4,326	**0**
Miscellaneous	0	0	0	**0**
Plot Fees	4,200	4,368	4,543	**0**
Total	66,378	69,032	71,795	**0**

Footnotes:
[1] Matt Jones (0.25FTE, T. Melton 0.45 FTE).
[2] 34.1% (Matt Jones); 48.3% (Melton).
[3] Student 40 hr/wk for 16 wks.
[4]2.7%.
[5]Includes lab and field supplies.
[6]In state travel.

Objectives:

1. Develop and validate a demographic model for pear psylla to assess pesticide effects on population management.
2. Continue to collect validation data for demographic models for mites and aphids.
3. Development new fruit growth models for Honeycrisp, Fuji, and Golden Delicious.

Significant Findings:

- Psylla phenology is well defined at this point in time.
- The final changes will be incorporated into the pesticide-effects model for psylla by early winter.
- A preliminary model for the pear psylla parasitoid, *Trechnites psyllae* was developed, but it needs to incorporate other data and be finalized next year.
- The phenology of pear bloom has been estimated for swollen bud, bud burst, and bloom for the cultivars Bartlett, Bosc and D'Anjou. We will collect more data for next year to fill out some of the other stages and better define the bloom period.
- Analysis of rosy apple aphid and apple grain aphid phenology was completed, and we have developed a method that will allow us to make pesticide effects models for these two aphids. We will be putting these two models up on DAS for beta users this spring.
- Our two-spotted spider mite data shows that diapause coloration is not a good indicator of when reproduction starts in the spring; egg deposition occurs almost immediately in the spring.
- Predatory mites are found in large number in the ground cover during the spring and fall, but most appear to migrate up into the canopy in June and remain there until the start of August. Management of the ground cover during the spring or fall could thus disrupt integrated mite management in the current or following year.
- Work on the fruit growth models for Cosmic Crisp, Fuji, Jonagold, and Honeycrisp was completed this year.

Obj. 1. Develop and validate a demographic model for pear psylla to assess pesticide effects on population management.

Methods Pear Psylla. Phenology data for pear psylla were collected at five locations with low-intensity management; samples were taken twice a week from February until the end of October. The number of adults (winterform and summerform), eggs, and immature stages (instars 1-3 and instars 4-5) was determined from beat samples and shoot samples. Shoot samples were visually inspected before leaves were developed, and subsequently processed through the mite brushing machine as the leaves became close to full size. In addition, unbaited sticky yellow cards were placed in each orchard (8/site) to catch more adults as well as the pear psylla parasitoid, *Trechnites psyllae*.

Weather data came from the high-resolution historical data provided by daymet which provides data at 0.6 x 0.6-mile resolution as well as from data loggers placed in the orchard from the period 2016-2019. Data was fit by maximum likelihood to five different statistical distributions and examined for the best overall fit across the range.

Methods Pear Bloom. Pear bloom phenology was evaluated at four locations with the cultivars Bartlett (3 locations), Bosc (1 location), and D'Anjou (2 locations). At each location we evaluated 60 fruiting buds (4 buds per tree from 15 randomly chosen trees – one bud per quadrant of each tree) and classified them as dormant, swollen bud, bud burst, green cluster, white bud, bloom, and petal fall. We visited each location twice per week to evaluate the clusters. Data analysis was done for each cultivar by using a maximum likelihood fit to one of five statistical distributions: (normal, lognormal, gumbel, gamma, Weibull).

Results and Discussion.

Pear Psylla Phenology. We completed evaluation of the pear psylla model for the winterform and summerform adults, eggs, early instars (1-3), and late instars (4-5) (Fig. 1). Our model shows that psylla begin laying eggs almost immediately – the adult and egg stages overlap almost completely when plotted on the same graph. We saw some variation in the late instars near the end of the season compared to the other stages, which was actually caused by a slight difference in DD between the sites at the end of the season. One of the changes compared to last year is that we found that the phenology was better estimated using a horizontal upper threshold for development.

Fig. 1. Phenology of pear psylla egg, early instars (1-3) and late instars (4-5). Dashed line is model predictions, circles are observed.

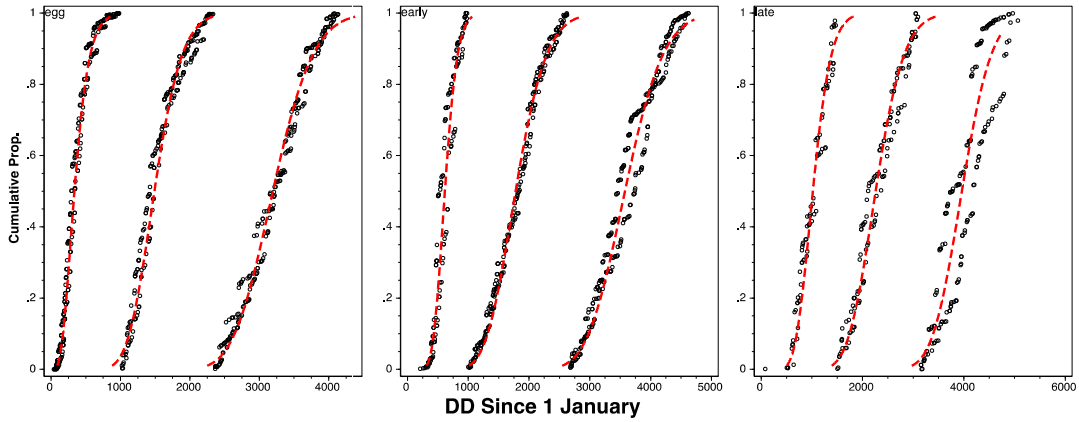

We have also already finished the first version of the pesticide effects model for pear psylla. The model needs to be updated for the data and changes we made this year, but we should have that done by the research review. We have made this model available to Dr. Louie Nottingham and will work with him to evaluate the optimal control strategies for pear psylla.

We have also made a preliminary model for the pear psylla parasitoid, *Trechnites psyllae* (Fig. 2). The yellow panel data showed very large numbers of *Trechnites* present which were used to make the preliminary model. We have additional data from our SCRI grant that would need to be added to this data and a larger evaluation of the literature on *Trechnites* needs to be made before we finalize the model.

Fig. 2. Phenology of trap catch of adult *Trechnites psyllae*. Dashed lines are preliminary model predictions, open circles are observed data.

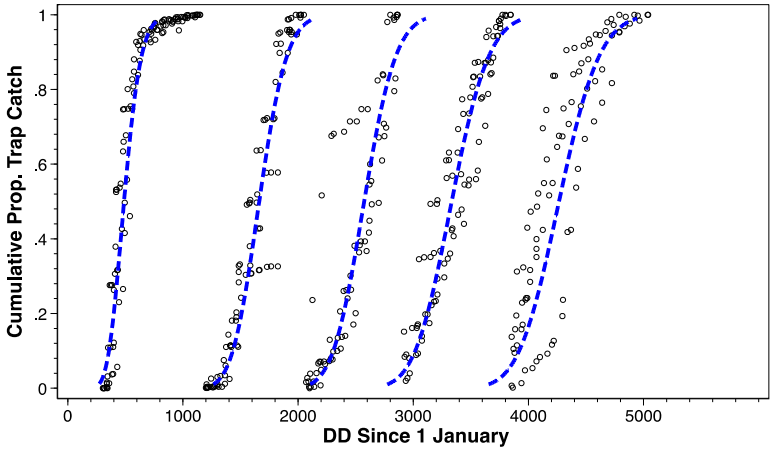

Pear Bloom. This is the second year of collecting data on pear bloom for the three cultivars. We were able to fit the data for swollen bud, bud burst, and bloom. The data for white bud and green cluster were not well represented by our sampling because the stages are so short that we were not able to get enough of a sample size to give us good estimates of the distribution of time over which they occurred. The different stages were all fit to a gamma distribution, which allows us to estimate the timing and percentage of the stages that are completed at any time (Fig. 3).

Fig. 3. Cumulative percentage through a given stage for 3 cultivars and 3 stages of pears. Based on data from 2018-2019.

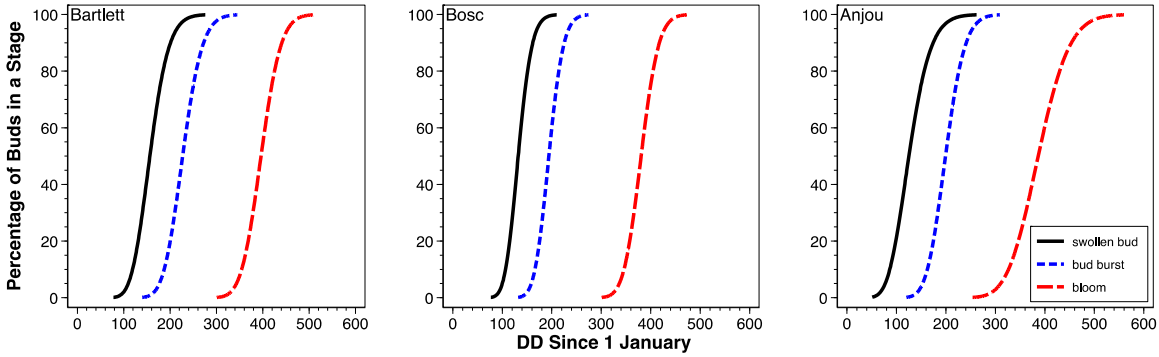

Work next year. Work on the pear psylla model is complete and the pesticide effects model modifications will be done in early winter. The *Trechnites* model needs to be further researched, but it appears that we already have enough data for making and validating the model both from this grant, and from our SCRI grant.

Next year we will collect more data on the bud stages so that we can better define some of the shorter stages (green cluster and white bud). These data should allow us to complete the bud model.

Obj. 2. Continue to collect validation data for demographic models for mites and aphids.

Methods. Phenology data were collected for woolly apple aphid (WAA), green apple aphid (GAA), two-spotted spider mite (TSSM), European red mite (ERM), and brown mite (BM). For GAA and WAA, four apple orchards were sampled twice a week from the end of March to mid-October. We sampled 100 shoots early in the year and 100 leaves later in the year (10 randomly chosen per 10 randomly chosen trees. The number of nymphs, nymphs w/ wing buds, wingless adults, and winged adults was recorded for each aphid species.

Phenology data for ERM and BM were collected from six apple orchards, twice a week from start of April until late-October. Initially, when eggs started to hatch, double-sided sticky tape was placed tightly around 50 branches per site (1 per tree) to detect mobile immature stages. After leaves expanded, a total of 100 leaves from 20 trees per site were collected and run through the mite brushing machine. Mite numbers were recorded by species and stage. In addition to the canopy samples, we also collected mites from the ground cover. Our results from last year showed that common mallow (button weed) consistently had high numbers of TSSM, so all the ground samples focused on that plant.

Results and Discussion

Rosy apple aphid & apple grain aphid. The phenology of rosy apple aphid and apple grain aphid from 2015-2017 were quantified and a model was developed that allows us to narrow the windows of when the aphids are in the orchard (shown in last year's progress report). We were concerned initially that we would not be able to make pesticide effects model for these species because of the rapid reproduction and quick overlapping populations. However, the limited time that they occur in the field showed us that we can use an additive variance model to show that the observed distribution

of aphids in the field reflects a total of three generations and that we can use this model to make pesticide effects models for both species. We have also provided the RAA and AGA phenology models to our programmer and should have them on DAS for beta users this year.

Green apple aphid. Analysis of the green apple aphid showed no big drop off related to temperature as occurs with WAA (reported last year). There is a significant reduction in immature survival during peak heat, but adults do not seem to drop off as much, so that recovery is quick. Part of the problem with GAA is that populations in the orchards build up significantly before any heat-induced mortality and thus the populations stay high throughout the season. While more analysis will be performed using our data, it does not appear as if we will be able to quantify phenology to any significant degree as we have with the other aphid species.

Mites. Our work on mites has focused on both emergence times and whether we can develop a model that simulates what we observe in the field. We have examined both European red mite (ERM), Brown Mite (BM), and two-spotted spider mite (TSSM). TSSM analysis is the furthest along and previously showed that the diapause-mediated color change (adult females turn orange when in diapause and return to greenish-tan when out of diapause) could be predicted by the daylength. The TSSM overwinters as adult females in reproductive diapause (if the temperatures are warm, they can feed or move about, but they are not reproducing until the temperatures & photoperiod rise above a certain level). Above 15.5 hours of light (roughly 1 May depending on site), we found the proportion of the adult female population switched relatively quickly to non-diapausing females (Fig. 4). However, we had also been taking leaf samples in the orchard and we found that eggs were produced at roughly the same rate per female when the female population was solely showing diapause coloration versus just after the female population showed no diapause coloration. Obviously, diapause coloration is not a true indicator of female reproductive status and cannot be used to guide management tactics for TSSM.

Fig. 4. Percentage of females showing diapause coloration and the percentage of the total eggs found before July 1 during the early season using data from 2017-2019.

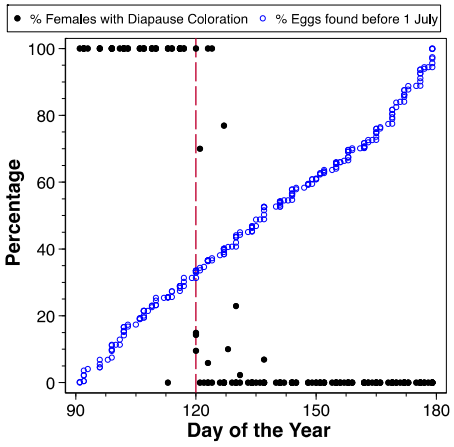

During the studies of TSSM, we have examined both ground cover weeds (primarily button weed which is an excellent host) and sampled the canopy for all stages as well as for the presence of predatory mites. Our data for the predatory mites shows that we have a fast early season build up in the weeds from early April through the end of May, a drop off during the period of June through the first week of August, then a large build up until the end of the season. At first, we though the drop off in mid-season was related to high temperatures that start about that that time, but examining the canopy samples, that period is the same as when a large increase in predatory mites were collected in the canopy. This suggests there is a net migration upwards from the ground cover and that ground cover effects are key to making sure that predatory mites are available when spider mite populations in the canopy are peaking. Timing of weed control is therefore as critical with predatory mites as it is with TSSM.

Work next year. This winter we will also program the RAA and AGA pesticide effects models and put them up on our current web site (pesticides.decisionaid.systems) so that users can evaluate the different control strategies. We will also perform more analysis on the GAA data to evaluate our models.

Mite work next year will probably not involve more data collection, but will concentrate on our analysis, especially on the early hatch of ERM and BM, but also the demographic models for all three species.

Obj. 3. Development of new fruit growth models for Honeycrisp, Fuji, and Golden Delicious

Methods. We collected data from 11 geographic areas representing the topographic and climatic diversity of Central Washington production areas from Brewster Heights to North Pasco. We concentrated on Golden Delicious, Fuji and Honeycrisp, but also collected data on Cosmic Crisp at the WSU Sunrise location. After early drop was completed, we tagged fruit and then measured the same fruit each week until harvest. Each fruit measurement was recorded separately, so that we could assess how the individual fruit size changed over the course of the season. We analyzed the data as the proportion of the final fruit size for each fruit, so that we don't have to worry about the effects of thinning, fruit load, or return bloom size. This method allows us to predict when the fruit reaches a given percentage of the final fruit size. The fruit size data was paired with temperature data, and degree days from 1 January (base temperature 40.1, upper threshold 75.7).

Results. Our average fruit growth data showed good agreement for most sites and cultivars for 2017-2019. The one variable site was in south Orondo (near Baker Flat) where the orchard was on a south facing slope that probably affected the Fuji grow size estimates by being warmer – this showed the same problem in 2017 and 2018 (black dots) (Fig. 5). The Honeycrisp data from 2019 at the Mattawa location in 2019 where the fruit growth appeared delayed (black dots) compared to all the others (Fig. 5). Because these sites were so anomalous, we dropped them from the final predictive model. These models will be available on DAS this coming year.

Work next year. There are no plans to continue this part of the project next year.

Fig. 5. Fruit growth throughout the season versus model predictions for each cultivar. Black solid circles indicate areas with anomalous data from South Orondo (Fuji) and Mattawa (Honeycrisp in 2019).

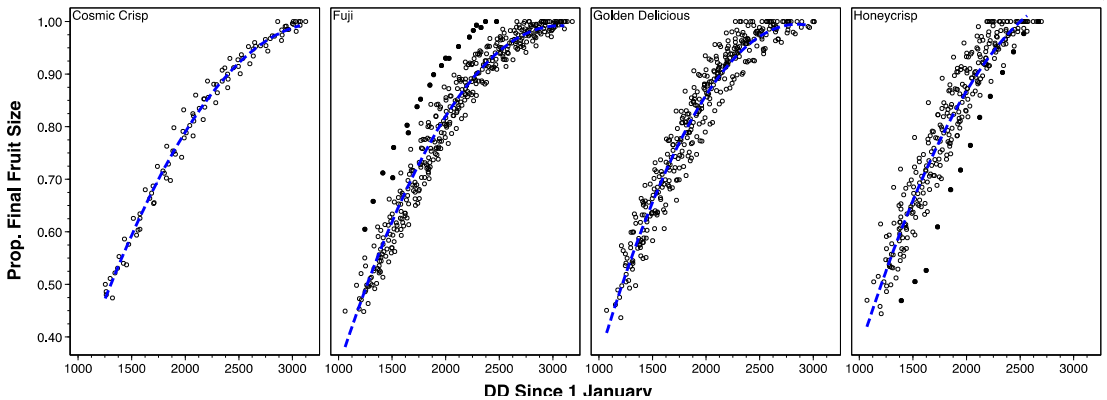

CONTINUING PROJECT REPORT **YEAR**: 2

WTFRC Project Number:

Project Title: Multi-purpose robotic system for orchards

PI: Avi Kahani B.Sc.
Organization: FFRobtics Ltd
Telephone: +972 5456 15020
Email: avikahani@ffrobotics.com
Address: 1b Yitzhak Rabin Street
City/State/Zip: Qadima Zoran Israel 4282300

Co-PI (2): Yoav Koster M.Sc.
Organization: FFRobtics Ltd
Telephone: +972 5287 37271
Email: yoavkoster@ffrobotics.com
Address: 1b Yitzhak Rabin Street
City/State/Zip: Qadima Zoran Israel 4282300

Co-PI: Manoj Karkee
Organization: Cetr for Precision & Automated Ag Systems, Washington State University
Telephone: 509-786-9208
Email: manoj.karkee@wsu.edu

Co-PI: Qin Zhang
Organization: Cetr for Precision & Automated Ag Washington State University
Telephone:
Email: qinzhang@wsu.edu

Cooperators: Columbia Fruit Packers, Auvil Fruits Inc.

Total Project Request: **Year 1:** 248,058 **Year 2:** 250,780 **Year 3: 255,692**

Percentage time per crop: Apple: 100% Pear: Cherry: Stone Fruit:

Other funding sources: None

Budget 1
Organization Name: FFRobotics Contract Administrator: Avi Kahani
Telephone: +972 545615020 Email address: avikahani@ffrobotics.com

Item	2018	2019	2020
Salaries	$59,400	$63,000	$66,150
Benefits	$5,940	$6,300	$6,615
Wages	$30,450	$31,500	$33,075
Benefits	$3,045	$3,150	$3,308
Equipment	$25,000		
Shipping (**)		$10,000	$10,000
Supplies	$12,000	$8,000	$6,000
Travel (*)	$20,000	$21,000	$22,000
Plot Fees			
Miscellaneous (***)	$10,000	$25,000	$25,000
Total	$167,950	$167,950	**$172,148**

Footnotes: Footnotes: (*) Travel budget is requested to cover the travel and accommodation (Travel from Israel)
(**) Shipping product to field experiments (***) Equipment

Budget 2
Organization Name: Washington State University **Contract Administrator:** Katy Roberts
Telephone: (509) 335-4564 **Email address:** katy.roberts@wsu.edu

Item	2018	2019	2020
Salaries	$53,522	$55,662	$57,889
Benefits	$5,101	$5,304	$5,516
Wages	$6,000	$6,240	$6,490
Benefits	$600	$624	$649
Equipment			
Supplies	$12,000	$10,000	$8,000
Travel *	$5,000	$5,000	$5,000
Plot Fees			
Miscellaneous			
Total	$82,223	$82,830	**$83,544**

Footnotes: *Travel budget is requested to cover the mileage for field experiments and to visit collaborators/co-PIs

1. OBJECTIVES

The following are the project objectives that remained same as the ones proposed in the original proposal.

1) Optimize camera configuration for multi-arm operation of our robotic harvesting machine
2) Integrate and demonstrate multi-arm harvesting robot to cover entire tree height
3) Evaluate the performance of the harvesting robot while in motion
4) Demonstrate integration of the harvesting robot with fruit conveying and bin filling system
5) Investigate machine vision and robotic end-effectors for blossom and green fruit thinning

1.1 Timeline of the Project Activities

Obj. #	Research Activities	Time					
		Year 1		Year 2		Year 3	
1	Develop a robotic system with multiple cameras						
	Optimize camera locations and create fruit map for harvesting based on accessibility				(1)		
2	Develop and evaluate a robotic harvesting system with multiple arms for entire tree						
3	Develop a control system for automated forward motion control						
	Evaluate the machine for automated operation during motion						
4	Integrate multi-arm robot with a harvest aid platform						
	Evaluate the performance of the machine for harvesting, conveying and bin filling						
5	Develop machine vision system for flower and green fruit detection						
	Preliminary evaluation of a robotic system for flower and green fruit						

There is a minor change in the schedule projected at this time. In the table above, **gray** cells represent the original schedule while **green** cell added at the end of second activity for objective 1 shows a minor change this time.

2. SIGNIFICANT FINDINGS

The most important accomplishment this year is that we were able to build a full-scale working system and evaluate it in Washington: . A YouTube video of the trial in the field can be found at https://youtu.be/YUdqTov9GeU. The trials in Washington exposed us to new apple varieties (Ambrosia, Honeycrisp, Kanzi) which added substantial and significant amount of data in our continuing efforts to improve the FFRobot.

- The deep-learning fruit detection algorithm worked properly, and showed promise for detecting obstacles such as branches and trellis wire.
- The multi arm system was working properly.
- The current robotic system is taller and wider than many commercial orchards; Consequently, we introduced design improvements of the structure of the system to support different

orchard structure, including netting, to be tested in the next (2020) harvesting season in Washington.

- The picking mechanism needed to be further optimized through:
  - Incorporating improved vision, path planning and navigation algorithms
    - Improving the mechanical design to support 10 feet rows AND detach ~~need to narrow the system to support the 10 feet rows~~
    - ~~Improving the harvesting mechanism to detach~~ the fruit with the stem.

- Results with blossom detection algorithm showed great promise for accurate detection

3. METHODS

Harvesting Objectives 1 to 4:

3.1 Obj.# 1: Optimize camera configuration for multi-arm operation of robotic harvesting machine

Introduction: FFRobotics first developed a robotic apple harvesting machine and in 2017 field tested it with one robotic arm (simple, linear actuation) with a single picking hand in conjunction with a single camera attached to the platform (https://www.youtube.com/watch?v=Dfu6jm6AHFQ). Together with WSU we found out that, in a modern fruiting wall orchard, more than 95% of apples can be detected (e.g. Silwal, 2016). Adding additional robotic arms (12 arms by now – tested in Washington) made it necessary to evaluate the optimal location of the camera: On the platform OR alternatively on the base of each robotic arm to achieve best data acquisition results. WSU team has been leading this objective in collaboration with FFRobotics team.

Materials: The current vision system has been modified to facilitate placement of the required hardware on the base of the robotic arm which is attached to the platform frame. Field data was collected to determine the percentage of apples detected by the vision system from different locations. The system has been and will continue to be evaluated in different kinds of orchards including -

(A) An orchard with fruit thinning to singles and pruning tree growth to approximately 10 inches beyond the trellis wires.
(B) An orchard with mechanical pruning
(C) Different canopy architectures including V-shape and Tall Spindle system.

Procedure: The entire image acquisition process begins by scanning the canopy directly in front of the initial multi-arms robot position. As some apples were blocked by other apples, leaves, branches, trunks and trellis wire - therefore difficult to be accessed and picked by robotic hand - a deep-learning-based image processing technique is being used to identify all potentially obstructing objects. This technique was able to detect apples that are not obstructed by the foregoing objects. These fruits - identified as completely visible and accessible may freely be picked by robotic hands. After the initial picking cycle is completed, the same section is re-scanned to see if more fruit are exposed with desired level of visibility and accessibility. The process is repeated until no accessible fruit are left. The picking system then moves down the row and the process is repeated. Missed apples were hand counted and compared to the number of detected apples. For vertical trees, this process can be repeated from the other side of the canopies to maximize the fruit harvesting percentage. The technique has been also extended to process videos collected by moving machine, potential improvement in fruit detection through different viewing angles.

3.2 Obj.# 2: Integrate and demonstrate multi-arm harvesting robot to cover entire tree height

Fig. 1: Multiple robotic arms supported by one frame

Introduction: As discussed in Obj. #1, the first prototypes - based on one arm - limited the ability of the robot to pick the entire tree. hardware and software changes were introduced to enable the dynamic structure of several robotic arms to gain the full range of 3 feet width, 3 feet depth, and 12 feet height canopies. Such a system was built and evaluated) in Israel during 2018 harvest season and an improved machine was evaluated in Washington in 2019 season. FFRobotics team has been leading this research activity in collaboration with WSU team.

Materials: Hardware and software have been modified to support the multi robot arms (6 robotic arms on each side) allowing dynamic movements along the height axis of the tree (Fig. 1). The new software algorithms control the entire system to allowing dynamic coordination between arms in term of their work-space.

Procedure: The image acquisition and processing system (described in Obj.#1) provided coordinates of linearly accessible fruit in the entire work space of the machine (which is roughly 3ftx3ftx12ft). Optimization techniques were employed to provide sequence of fruit to be picked by each arm of the multi-arm robotic system. To optimize the system, more experiments were and will be carried out by sending (but not picking), the robotic arms to the desired fruit. This experiment will allow evaluating several techniques of sequencing fruit picking pattern in the same location.

3.3 Obj.# 3: Evaluate the performance of the harvesting robot while in motion

Introduction: Hardware and software changes were introduced to automatically move down the row in optimal steps as per the progress in fruit picking estimated by the camera system. FFRobotics team is leading this research activity in collaboration with WSU team.

Procedure: The operation begins by scanning the canopy to detect the fruits,and followed by the picking process, automatically moving to the next stop. During the field evaluation, machine capacity, percentages of picked and bruises apples, time between the consecutive locations and the time to stabilize the robotic frame to be ready for the next picking session were and will be collected. The picking system will then move down the row by certain distance (e.g. 1 meter; based on the frame structure) and the process will be repeated.

3.4 Obj.# 4: Demonstrate integration of harvesting robot with fruit conveying and bin filling system
Introduction: Picking system and the Harvesting Aid platform were integrated and evaluated to demonstrate bruise-free end-to-end, fully functional harvesting solution.

Materials/Procedure: 6 robotic arms in the same frame allow dynamic movements along the height of the tree as an add-on on an existing Harvesting Aid System (Automated Ag. Platform). The integration of Harvesting Aid platform and multi-robot conveyer system presents end-to-end solution from tree-fruit harvesting through to conveyance all the way to the bin. FFRobotics and WSU teams are co-leading this research activity.

Blossom and Green Fruit Thinning Objectives 5:
3.5 Obj. #5: Investigate machine vision and robotic end-effectors for blossom and green fruit thinning

Introduction:, Blossom and green fruit thinning will be another crucial step requiring automation or robotic solution. Concurrently with the present project, , some efforts is placed on robotic blossom and green fruit thinning. Our hypothesis is that, in the long term, all the manual operations in the field need to be automated and the machines need to be multi-functional with plug and play capability. WSU team is leading this objective in collaboration with FFRobotics team.
Materials: A multi-camera system was developed and used (Obj.#1) above for detecting accessible

fruit for harvesting. The same cameras and sensors are/will be used to collect images from apple orchards during bloom and green fruit stages. The images are analyzed to detect and localize flowers and green fruit, and a robotic system (the same as described in Obj. #2), will be used to approach targeted flower and green fruit cluster for destroying or removing desired amount of flower and green fruit.

Procedure: In this work, the deep learning algorithm developed in Obj. #1 has been revised and improved to detect flowers during the bloom stage, and will be extended to detect green fruit as early as possible. Flower and green fruit locations will be estimated using a stereo-vision system of two cameras installed slightly offset to each other. Flower or green fruit location will be provided to the robotic machine (the same machine as in objective #2, with new end-effectors/hands developed for thinning) removing unnecessary flowers or green fruit. Various end-effector technologies - including pressure hose, waterjet, electrically actuated brush system – are evaluated for best effectiveness.

4. RESULTS & DISCUSSION

4.1 Obj.# 1: Optimize camera configuration for multi-arm operation

Images and videos have been collected and are being processed for improved detection and localization of apples for fruit harvesting. Data were collected using an Intel RealSense 435 camera (Intel, USA) mounted on top of a robotic arm moving across its workspace. Video processing has a potential to provide additional visual perceptions for detecting occluded apples and those in clusters through a sequence of frames that provide varying viewing direction to the overlapping canopy areas. In addition, the machine vision system, developed using a Mask RCNN (one of the latest deep learning techniques), was expanded to detect additional parts of tree canopies including branches and leaves along with fruits, so that important orchard characteristics such as branch obstruction, occlusion and pseudo-pendulum effects can be detected, Fig. 2.

Fig. 2: Apples marked in the image are identified to be safe to harvest in the given view. For each of these pickable apples, the

The proposed method detected fruit parts with a mean average precision (mAP) value of 87% on a test dataset. The binary mask obtained for each class from Mask-RCNN output was further analyzed to provide safe (avoiding apples that are occluded or not safe to pick for the given view) and reliable (providing right picking orientation by considering the fruits immediate surrounding) harvesting decision to the robot. With this proposed approach, the system was able to identify apples that were safe to harvest with 92% accuracy and was able to predict the fruits difficult to harvest with 91% accuracy compared to ground truth data. Though current robotic system for picking may not utilize the variable approach direction, new capability of the vision system provides an opportunity to improve the overall harvesting system in the future.

In addition to branches and other fruit, trellis wires also present significant obstacles to robotic picking and thinning. Trellis wires were only partially visible (in segments) in images due to their thin size, and occlusion due to branches and leaves. A trellis wire detection technique was developed utilizing binary line descriptors and Haar-like features were combined at the decision level. Segments of the trellis wires detected by the vision system were combined using Hough Transform so that wire location could be estimated in the occluded regions as well. Preliminary analysis showed the trellis wire detection F1-score of 83% (Fig. 3). This technique can be integrated with the current robotic harvesting system to avoid robot collision with trellis wires.

Fig. 3: Trellis wire and trunk detection to avoid end-effector and trellis wire collision. Even though only parts of the trellis wire are visible, the algorithm can reliably estimate the occluded part of the trellis wire assuming a linear geometry.

The additional information gained with the improved algorithms, and the improved mechanism (additional degree of freedom – controlling the twist of the gripper), allowed us to catch the fruit based on the stem orientation and to twist each fruit based on its specific/particular orientation. Based on the tests this year, it is clear that additional optimization is necessary on these algorithms, as in too many cases (~27%; Fig. 4) fruit was picked together with small brunches and 44% were picked without stem. During the tests we already introduced a different method that we believe can improve the result significantly. During the harvesting tests in Washington, we faced a major issue related to obstacles and understanding what we term a "blocked apple". "Blocked Apple" - an apple which we identified as one we cannot reach – the definition was too narrow: In fact, we identified numerous cases which made it apparent that the meaning of "Blocked Apple" should be wider and include all cases in which picking one apple will cause loosing other apples in its near vicinity.

Fig. 4: Sample apples harvested by the

We took more than 20K images to train the system with better understanding of the 3D location of trellis wire and the fruits. Which was used in the algorithm discussed earlier for trellis wire detection. Based on the feedback from the growers we add a sorting / clipping station ("table") before the bin filler to enable the growers to implement manually the sorting / clipping before we automate this part.

Fig. 5: Full scale robotic

Fig. 6: End-to-end system developed for robotic fruit harvesting, conveying and bin filling.

Objective 2,3 and 4: Full-scale, integrated robotic system development and evaluation

As discussed before, this year, we designed a full scale robotic harvesting systems (Fig. 5 and 6). The robotic picking system was integrated with a Bin Carrier from Automated Ag Systems and a Bin Filler from Maf Roda Industries, for evaluating the completed (end-to-end) harvesting process. The Prototype used in the field trials in Washington allowed us – in parallel - to design together with Automated Ag and Maf Roda - the final platform that will be the base for the commercial system

keeping the same method of operation in the field as done today. The performance of the entire system was not tested in full.

Obj. #5: Investigate machine vision and robotic end-effectors for blossom and green fruit thinning

The effectiveness of automated/robotic thinning significantly depends on blossom detection and estimation of spatial distribution of blossoms under varying background and lighting condition. In order to detect blossoms, a deep learning (Mask R-CNN) based unified semantic segmentation architecture was used. The algorithm takes single image as an input and returns all the instance of flowers/blossoms at pixel level for precise localization of blossoms. Additional images were collected from commercial apple orchard in WA during hand blossom thinning in daylight condition without background manipulation. The image dataset constituted more than 200 images with ~10,000 blossom instances. Mask R-CNN based deep learning algorithm was powerful in learning features of blossoms and was capable of correctly performing pixel level detection of blossoms in images that were never seen by the deep learning model before. Fig. 7 shows the comparison between the human labelled ground truth (blue polygons) and detection results (red polygons) achieved by Mask R-CNN algorithm. Furthermore, with the additional dataset, it was observed that blossom detection in deep learning algorithm was minimally affected by background sky which happens to have similar appearance as blossom. The system achieved a mean average precision (mAP) of 0.86 in detecting blossoms in apple trees.

Fig. 7: Detection result achieved by Mask R-CNN algorithm compared with ground truth dataset. Objects inside blue, and red polygons indicate ground truth and detection results respectively (a) Scifresh apple blossoms (b) Envi apple blossoms. MaskRCNN was robust enough to detect true

In 2019, we also put our efforts toward development of thinning rules for robotic thinning applications. We employed Convolution Neural Network (CNN)-based technique to estimate spatial distribution of blossoms, Fig. 8. In order to account for blossoms with varying cluster size, a multi-column convolution neural network was employed to improve the prediction accuracy for different cluster size. Preliminary analysis showed that the algorithm can achieve a Mean Absolute Percentage Error (MAPE) of 62% in counting blossoms in test datasets. Further improvement in estimation of spatial distribution of blossoms would be valuable for improving the estimation accuracy and developing thinning strategies/rules.

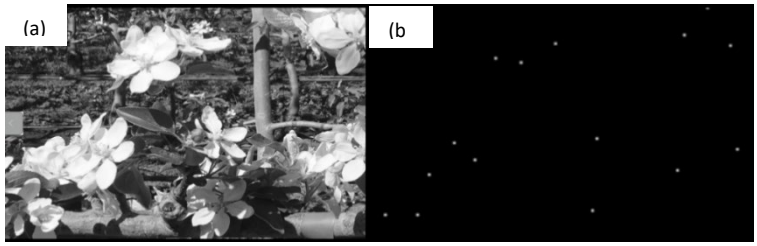

Fig. 8: (a) Monochrome image of apple blossom (b) Corresponding spatial distribution of blossom centroids detected by deep learning algorithm

Furthermore, we investigated and evaluated the performance/efficiency of multiple off the shelf end effectors for blossom removal. We tested operation of pneumatic hose (pressurized air), Waterjet (high velocity pressurized water), and electrically actuated brush system, The pneumatic hose and waterjet were ineffective; often dragging the remaining blossoms on the water/air flow direction and badly affecting surrounding blossoms that need to be saved. Electric brush system, while effective in some occasions, did not easily engage with the blossoms often rotating and weakening the stem during operation. Based on the experimental evaluation, we designed an electrically actuated end effector with rotating blades/string spaced apart, which will be further developed and evaluated in the next year Fig. 9.

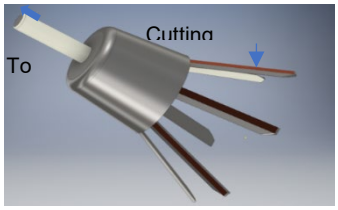

Fig.9: Proposed electrically actuated end effector system. Shape is designed conical shape to save important flowers while removing unnecessary

Green Fruit Thinning: Upon analysis of RGB images for green fruit detection, it was found that segmentation of green fruit from apple orchards would be challenging in visible spectrum. Green fruits happen to have similar appearance as apple leaves hence limiting the number of features that can be useful for segmenting green fruit. This year multispectral image data were collected during green fruit thinning season. Multispectral images have clear advantage over RGB image as more spectral information are available. The collected images will be processed in future for green fruit detection and localization.

CONTINUING PROJECT REPORT **YEAR**: No-cost extension

Project Title: Towards automated canopy and crop-load management in tree fruit

PI: Manoj Karkee
Organization: Washington State University Center for Prec. & Automated Ag. Systems (WSU CPAAS)
Telephone: 509-786-9208
Email: manoj.karkee@wsu.edu
Address: 24106 N Bunn Rd
Address 2:
City/State/Zip: Prosser, WA 99350

Co-PI (2): George Kantor and Abhisesh Silwal
Organization: Carnegie Mellon University Robotics Institute
Telephone: 412-268-7084
Email: kantor@ri.cmu.edu
Address: 5000 Forbes Avenue
Address 2:
City/State/Zip: Pittsburgh, PA 15213

Co-PI(3): Mathew Whiting
Organization: Washington State University Center for Prec. & Automated Ag. Systems (WSU CPAAS)

Cooperators: Curt Salisbury, Abundant Robotics Inc.; Dave Allan, Allan Brothers Fruits; Karen Lewis, Washington State University

Total Project Request: **Year 1:** $115,904 **Year 2:**$80,740 **Year 3: 0**

Percentage time per crop: Apple: 80% Pear: Cherry: 20% Stone Fruit:
(Whole % only)

Other funding sources

Carnegie Mellon University has a project scientist working on this project. Only a small fraction of their salary has been requested as per Budget 2 below. Remaining funds for the scientist's involvement will be covered by the university through other funding sources.

WTFRC Collaborative expenses: None

Budget 1
Organization Name: Washington State University **Contract Administrator:** Katy Roberts
Telephone: (509) 335-4564 **Email address:** katy.roberts@wsu.edu

Item	2018	2019	2020
Salaries[1]	$27,653	$28,759	
Benefits[1]	$ 2,303	$ 2,395	
Wages	$13,500	$14,040	
Benefits	$2,448	$2,546	
Equipment			
Supplies[2]	$3,000	$3,000	
Travel[3]	$1,000	$1,000	
Miscellaneous			
Plot Fees			
Total	$49,904	$51,740	$0 (no cost extension)

Footnotes:
[1]Salary and benefit for a PhD student

[2]Cost to purchase sensors, metals, and other supplies for lab and field tests
[3]Travel cost for field data collection, and testing; and travel cost for cooperative meetings

Budget 2

Organization Name: Carnegie Mellon University **Contract Administrator:** Patricia Clark
Telephone: 412-268-3483 **Email address:** pclark@andrew.cmu.edu

Item	2018	2019	2020
Salaries[1]	$0.00	$5,000.00	
Benefits[1]	$0.00	$1,170.00	
Wages	$0.00	$0.00	
Benefits	$0.00	$0.00	
Equipment	$66,000.00	$18,454.11	
Supplies[2]	$0.00	$1,300.00	
Travel[3]	$0.00	$3,000.00	
Miscellaneous	$0.00	$75.89	
Plot Fees	$0.00	$0.00	
Total	$66,000	$29,000.00	

Footnotes:
[1]A part of salary and benefit for a project scientist
[2]Cost to purchase sensors, metals, and other supplies for lab and field tests
[3]Travel cost for field data collection, and testing; and travel cost of cooperators

1. OBJECTIVES

The following are the project objectives, which remain the same as originally proposed.

1. Formulate objective pruning rules by integrating pruning strategy desirable for robotic/automated harvesting and the strategy currently used by growers in fruiting wall apple (e.g. formally trained) and cherry (e.g. UFO) orchards;
2. Develop a machine vision system to locate pruning branches in those two crop architectures.
3. Integrate and evaluate a robotic pruning machine.

Timeline of Project Activities

Objectives#	Research Activities	Time (Calendar Years and Quarters)							
		2018		2019				2020	
		Q3	Q4	Q1	Q2	Q3	Q4	Q1	Q2
1	Develop pruning rules								
	Identify pruning branches								
2	Acquire canopy images and create 3D structure of trees								
	Investigate potential for dead branch and flower bud detection								
3	Evaluate integrated pruning robot								

2. SIGNIFICANT FINDINGS

1. Professional pruners/managers consider formal guidelines when identifying pruning branches in dormant apple canopies. In practice, however, the branches pruned by professional pruners were inconsistent with stated guidelines and demonstrated substantial amounts of variability.
2. Deep learning techniques are capable of analyzing canopy images to estimate various parameters such as size and location of branches.
3. Our integrated pruning system is capable of pruning branches at manually selected cutting points. Autonomous selection of cutting points and a field experiment planned for spring 2020.

3. METHODS

3.1 Objective #1: Pruning Rules and Pruning Branch Identification (Carnegie Mellon – Lead; WSU Participant; Abundant Robotics Collaborator)

In the past it was found that, for the tall spindle tree architecture, the pruning process can be captured by four basic rules (Karkee et al., 2014); *i) remove diseased or dead wood/branches; ii) remove branches longer than a specified length; iii) remove branches larger than a specified diameter; and iv) remove branches to maintain a specified spacing.* Lehnert (2015) proposed eight rules for pruning tall spindle apple trees, some of which were similar to four different rules proposed by Karkee and Adhikari (2014). It was also claimed that two major rules; i) remove two to four largest limbs, and; ii) remove all vertically growing limbs (40 degree or less); will cover more than 90% of pruning job in tall spindle apple orchards. These previously developed rules are essential for automated pruning of tall spindle apple orchards.

However, more work is necessary to develop and apply pruning rules to identify pruning branches in other tree architectures including formally trained apple architectures. Engineers, horticulturists and growers have been working together to explore pruning methods for the proposed canopy architectures. Special consideration have been given to the desired limb and fruit distribution for

robotic apple harvesting that include the need of presenting fruit individually and without any obstruction by the branches, trunks, or trellis system.

Similar to Karkee et al. (2014), the pruning rule formulation process included observation and analysis of the work of experienced pruners and supervisors. Experienced pruners were selected from commercial orchard crews. They were asked to individually tag pruning branches on randomly selected fruit trees using unique color tags. To keep tagging independent between workers, tags were removed from the tree before another worker was asked to tag the pruning points on the same tree. Video and color images of each tagged tree were captured.

Pruning branches identified by workers as well as the total number of branches were located and counted for each tree. Videos and still images were analyzed to look for the pruning patterns and process each worker follows. A set of objective pruning rules are being defined using; i) expert's knowledge captured from engineering team based on their need for robotic harvesting; ii) horticulturists and growers based on their understanding of training practices, tree architectures, and physiology; and iii) from experienced workers based on pruning processes they follow. We have been visiting with different collaborators to get their input on the pruning strategies to support the process of pruning rule identification.

After objective pruning rules are defined, the 3D tree structure created in Objective 2 and pruning rules will be used to identify branches for pruning. For this task, a novel deep learning-based method is being used to distinguish trunk, main branches and sub-branches or laterals of a tree. Geometric parameters of tree canopies including branch size (diameter), branch length, and branch spacing will be estimated using the 3D measurements and corresponding color images. Once all the topological and geometric parameters of trunks and branches are estimated, decisions can be made using pruning rules to determine which branches need to be pruned.

3.2. Objective #2: Machine Vision System (WSU and Carnegie Mellon – Co-Lead)

Under this objective, we have been focusing on creating 3D structures of apple and cherry trees trained in modern fruiting wall architecture (e.g. formal training for apples, UFO architecture for cherries). Five major steps are involved in the generation of 3D structures of fruit trees and identifying pruning points; i) image acquisition; ii) Faster Region-based Convolutional Neural Networks (Faster R-CNN); (iii) Generative Adversarial Network (GAN); iv) point cloud generation; and v) combining (ii), (iii), and (iv). A stereo-vision camera, a laser sensor, and a Zed camera have been used to capture 3D information from trees. Stereo-vision system provided high-resolution 3D information, whereas laser sensor provided more accurate 3D location. Zed sensor also has the potential to provide equally accurate 3D information at lower cost. Comparison and fusion (when necessary) of 3D information from these sensors will lead to improved resolution and accuracy of 3D information of the trees. Stereo-vision camera also provided complimentary color images.

After image acquisition and 3D point cloud generation, a novel deep learning-based system was used to generate 3D structure of apple trees. A state-of-the-art object detection algorithm (F-RCNN) proposed by Ren S., et al. (2015) was used to identity branching points from color images. These branching points were strong visual ques that will be used to detect branch occlusion that would be necessary to segregate individual branches as a whole. The link between the detected branching points will be associated using skeleton image generated by the Generative Adversarial Network (GAN).

The output of the GAN was a binary image with an array of connected binary pixels that traced the mid-section of branches in the color images. A multi-channel GAN was used to generate skeleton image for branches and main trunk. Once the skeleton was identified, the curvature of the branches and trunk was warped using the depth information obtained in the previous steps to reconstruct the 3D models. Using this info, the length and size (diameter) of each branch are going to be estimated.

Length can be estimated using the starting and end points of the branches. To estimate diameter, the skeleton of the tree will be overlaid on top of the color images taken from the same perspective. Then, the number of pixels in the orthogonal direction of the branch skeleton will be counted at the base of the branch (2 to 5 cm from the branch-trunk junction). Resulting 3D skeleton and geometric parameters will be used in identifying pruning branches as discussed in Objective 1.

In addition to geometric parameters such as size and length, productiveness of a branch is another consideration for pruning. If a branch is dead or otherwise unproductive (without enough fruiting locations), it needs to be pruned out. Detecting if a branch is dead and estimating number of flower buds in live branches would be valuable information to make automated pruning more effective. This work will investigate the potential of using spectral signature (using a hyperspectral camera) to differentiate dead and live branches in the dormant season. When a dead branch is detected, the attribute of the branch will be updated in the 3D skeleton to indicate that the corresponding branch needs to be pruned out. Another task in this objective will be to investigate the potential of a machine vision system for flower bud detection and counting. This information will be important for both automated as well as manual pruning. Currently, many growers make decisions on pruning strategies based on number of flower buds before and after pruning so that desired level of crop-load can be achieved. Because the color, shape and size of flower buds will be similar to other parts of branches, automated detection will be challenging. We will explore the use of spectral signature in addition to geometric parameters to investigate its potential to address these challenges. We will also evaluate image resolution, viewing angle and computational power desired in detecting flower buds, which will help establish the potential for automated flower bud detection in dormant season.

3.3. Objective #3: Integrated Robotic System Evaluation (WSU–Lead; CMU Participant; Abundant Robotics Collaborator)

In the proposed work, various end-effector mechanisms are being developed and integrated with a robotic manipulator to carry out various specific tasks. The machine vision has also been integrated with the hardware system for complete system development and evaluation in lab and field environment. One of the end-effector being developed is a round cutter that can close around a branch. If everything around a branch needs to be removed (e.g. lateral branches in UFO cherries), this end-effector mechanism can be guided along the branch using the 3D structure of the trees developed earlier (Objective 2). A short saw-bar will also be developed and evaluated for removing all the secondary branches growing in a certain section of the primary branches. For example, everything growing longer than 6 inches below a horizontal limb in a formal apple orchard can be removed with this mechanism. Another end-effector being evaluated is a pair of scissors. This type of end-effector is being evaluated in cutting individual branches.

4. RESULTS & DISCUSSION

4.1 Objective #1: Pruning Rules and Pruning Branch Identification.

Our hypothesis for automated pruning rule generation was that the observation of commercial pruning operation and analysis of images/ 3D models captured before and after pruning could lead to objective pruning rules. To test this theory, we assigned professional pruners to follow commercially adopted pruning rules and prune forty dormant apple trees. For these canopies, the camera system was placed in a stationary location approximately one meter in front of the canopy and we collected before and after pruning wide angled stereo images. Later, point clouds from the two pre/post pruning datasets were overlaid to pinpoint individual cut points. Figure 1 shows this underlying concept.

A summary of the critical components of the ideal pruning rule for dormant apple trees are listed below for discussion. A detailed description of the pruning rule practices by professional pruners is included in our previous report.

- Use of a BCA tool (Fig. 2) to optimally determine the appropriate number of fruiting location per unit length of the lateral branches.
- Fruit spacing was considered an important parameter. Minimum fruiting zone spacing was approximately 4 inches as anything closer might lead to clusters of fruit during harvest season.
- Length of fruiting laterals was another important factor. Laterals longer than 8 inches were trimmed.
- Considerations were also made to remove vertical fruiting sites and those right over or under the horizontal branches.
- Selectively remove smaller buds from a cluster. Remove buds too close to the trellis wire, shoots under the branches, and vertical fruiting zones.
- Remove dead and diseased branches and tie shoots closer to the edge of the branch to fill gaps if lateral branches are short.

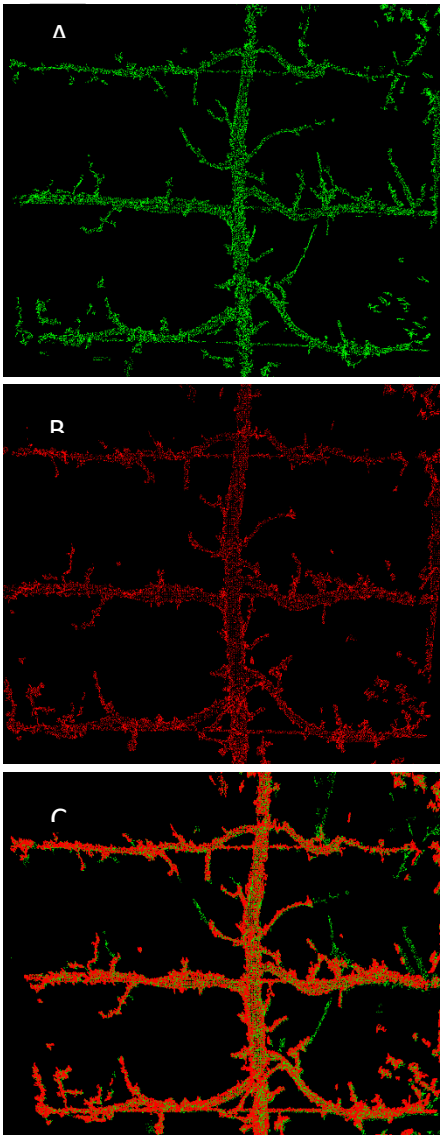

Fig. 1 Pre/post pruned point cloud overlay. (A) pre pruned point cloud. (B) post pruned point cloud. (C) overlaid point cloud. The intersections of green and orange points indicate cut points.

The analysis of the pre/post pruning data revealed inconsistency in following the strict guidelines for pruning apple canopies. In practice, branch diameters were assessed visually and intuitively without the use of the BCA tool. This led to suboptimal selection of number of fruiting location per unit length of the lateral branches. Additionally, the minimum gap between fruiting locations were estimated using the width of the palm as a unit of measurement which varied from one pruner to another. These differences between the ideal and practiced manual pruning lead to greater variation in the data for training a machine learning agent. Because of these recent revelations, we are currently focusing on synthesizing a pruning rule by just utilizing the geometric measurements and topological parameters. We realized that the most important aspect of pruning is the uniform distribution of fruit, therefore we intend to implement the following simplified pruning rule that prioritizes fruit distribution.

1. Estimate diameter and length of lateral branches and use the BCA equation to determine optimal number of fruiting locations per unit length of the lateral branches.
2. Count and measure the length of secondary branches and only keep secondary branches with minimum of 4 inches gap.

Fig. 2 Tool used to measure Branch Cross-Sectional Area (BCA)

4.2 Objective #2: Machine Vision System

The analysis of the pre/post pruning data demonstrated that a single view of the canopy was not enough to generate detailed 3D structure of the canopy. Secondary branches protruding towards and directly away from the camera were missing in the 3D structure when only one viewpoint was used. To mitigate this limitation, Co-PI Silwal from CMU

designed a new camera system that images the canopy with two stereo cameras systems (Fig 3).

Fig. 3 A multi-view stereo camera system. Camera system with linear slide imaging dormant apple canopies.

The new camera system has two stereo pairs, one at a lower height for front view of the canopy and another at a higher and angled position for the top view. Both top and bottom camera slide along the linear slider at three different locations and provides a total of six different views of the canopy. The stitched point clouds from six different locations provided a more detailed 3D structure of the canopy.
In addition to multi-view stereo, like its predecessor, this new camera system is also equipped with active lighting that generates consistent image quality regardless of ambient lighting condition. Figure 3 compares two images of the same canopy acquired using a cellphone (Fig. 4A) and the new camera system (Fig. 4B). In the cellphone image, background is cluttered with trees from adjacent rows, sky and ground which makes it harder for any computer vision algorithms to analyze the canopy in the foreground. In contrast to this, the image from our new system naturally highlights foreground keeping background darker and consistent. This active lighting-based camera system enables us to reduce variables in an unstructured environment with varying lighting conditions and functions a robust tool that is critical for generating accurate 3D model of the canopies.

Fig. 4 (A) Daytime image of a cherry orchard taken with cellphone; (B) Daytime image of a cherry orchard imaged with the new global camera.

To implement any pruning rule, the vision system should be able to estimate key aspects of tree canopies such as branch and trunk structures and sizes, and number and location of buds. Currently, we have implemented a variation of a deep learning technique called Generative Adversarial Network (GANs) that directly outputs a 2D skeleton image of just the secondary branches. This is advantageous over conventional computer vision algorithm as it bypasses several intermediate processing steps such as pre-processing, multi-class segmentation, and post-processing steps that could potentially add more inaccuracies. Currently we are investing our research efforts in utilizing the output of GANs to identify and localize cut point locations. This is being done by using simulated annealing which is a brute force optimization algorithm that explores all possible combinations until optimal solution is found. In our case, the optimal state is the state that minimizes the cost (here the cost being proportional to absolute difference of distance between two branches “d” and desired

distance between branches D, approximately equal to 4 inches). Result of automated pruning point identification and localization will be provided as an input to the integrated robotic pruning system.

4.3 Objective #3: Integrated Robotic System Evaluation

For Objective 3, our team is collaborating with Dr. Joseph Davidson from Oregon State University. A UR-5e robot arm from Universal Robots is being used for developing an automated fruit tree pruning system. This manipulator has demonstrated good speed, reach and maneuverability, and therefore has been acquired at both Collaborator Davidson's and PI Karkee's labs, which has facilitated collaborative system development, integration and evaluation. Developing an integrated software stack for robot control is key for a successful pruning system. Our approach includes the following:

1) Create a probabilistic 3D map of the orchard environment using Octrees (Fig. 5)
2) Generate collision free paths to the identified pruning points using RRT*, an established algorithm designed to efficiently search nonconvex, high-dimensional spaces
3) Execute a controlled approach to the cut point using inverse kinematics support available in MoveIt, an open source tool that provides motion planning, kinematics, control and navigation support packages
4) Cut the identified branch

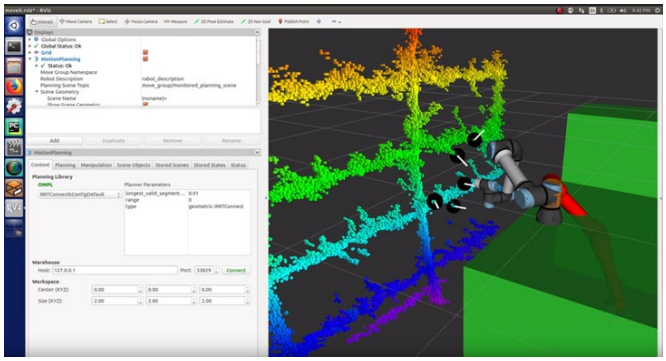

Fig. 5 Simulation of branch pruning in Gazebo. A 3D OctoMap of an apple tree has been created from a Kinect scan. Five pruning points were selected randomly. The UR-5e traces a collision free path found with RRT.*

During Summer 2019, we developed an integrated pruning system and evaluated its planning and execution performance in a lab environment. The pruning system is shown in Figure 6, consisting of the UR5e equipped with an end effector and an eye-in-hand Intel RealSense D435 camera. The end effector is a pneumatically actuated four-bar linkage with custom-ground blades. Initial tests showed the end-effector could consistently cut branches up to 10mm in diameter near the pivot point of the blades. The planning framework we utilized is called FREDS-MP, which aims to increase the planning speed and overall throughput of the robotic system. FREDS-MP works by precomputing a database of optimistic trajectories offline, utilizing these trajectories during the online phase as effective priors, and ordering the cut points more effectively.

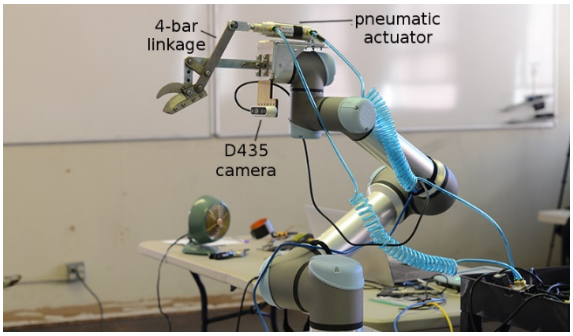

Fig. 6 Our pruning robot setup, consisting of a UR5e robot arm, an Intel RealSense D435 camera, and a custom pneumatically actuated pruning end-effector

Currently, given a set of manually selected cut points, our system is able to localize itself against the corresponding real tree, identify the corresponding points, and execute the pruning procedure. Our ensuing goal is to use 3D data acquired from a computer vision system to autonomously determine branch cut points as discussed in Objectives 1 and 2. Improvements are also being made on the scissors-type pruning end-effector currently being used. Our goal is to make the end-effector electrically actuated to increase the pruning capacity to 45mm diameter branches while keeping it lightweight. We are working to integrate a newly designed eye-in-hand stereo camera from CMU to replace the Intel RealSense D435 that has been used in the lab tests. This camera will provide higher quality 3D models of the tree as compared to the Intel RealSense, which will allow for more robust pruning. Lastly, we hope to complete a field evaluation of the integrated system by Spring 2020.